Spring 5-7-2014

Investigating Drift Mobilities in Cadmium Telluride Solar Cells

Daniel Goldman
Syracuse University

Abstract

Cadmium telluride thin film solar cells are the major competitors to thin film Silicon solar cells in today's solar cell market. However, many aspects of the physics behind CdTe solar cells still elude the scientific community, specifically electronic transport properties such as drift mobility. This project concerns the investigation of carrier drift mobilities in various thin film CdTe solar cell samples using a photocapacitance measurement technique. The physics describing semiconductors and solar cells is presented, as well as a description of CdTe thin film solar cells and drift mobilities. After describing the photocapacitance measurement, examples of the drift mobilities obtained from these measurements are exhibited. These results contribute to the idea that drift mobilities in thin film CdTe are orders of magnitude smaller than the values used by device modelers, which can have substantial implications on the performance of these devices.

Contents

0.1 Executive Summary

The most active field of contemporary physics research is not astrophysics or particle physics, it is condensed matter physics. Condensed matter physics is concerned with the study of various phases of matter, primarily solids and liquids, and the physical laws and properties which describe them. The field encompasses unique phases of matter such as superconductivity, and forms the basis of modern materials science. The multitude of material properties, such as electronic, structural, and optical properties, are measured and described by techniques founded in condensed matter physics.

One of the most important applications of materials science and condensed matter physics is in materials and technologies for alternative energy. For example, having lighter and more aerodynamic materials for wind turbine construction both reduces cost and increases the efficiency of the turbine system. Another important example, the focus of my Capstone project, is the physics of solar cells, one of the most promising technologies for alternative energy. Solar cells, also known as photovoltaic cells, are devices which convert light energy into electrical energy through the photovoltaic effect. The photovoltaic effect is the creation of a voltage or electrical current in a material due to its exposure to light. This basic principle drives solar cell

technology: extracting as much energy through sunlight as possible and converting it to electricity.

There are many different types of solar cells: from the silicon cells you see on roof panels to the thin film solar cells I worked with. Thin film solar cells are cells made by depositing one or more thin layers of photovoltaic material on a substrate, the semiconductor base on which the solar cell material is placed. One important material used for thin film solar cells is cadmium telluride (CdTe), which is a crystalline compound formed from cadmium and tellurium. CdTe photovoltaic cells are the main competitors to thin film silicon technology on the commercial solar cell market today due to their low cost and advanced technology. This makes technological advances in CdTe critical to the development of thin film photovoltaic technology as a whole.

Improving the solar to electronic energy conversion efficiency is a method commonly used to increase the performance of solar cells. One way to possibly improve the efficiency is by ensuring improved voltage capabilities through higher electron drift mobilities. Drift mobilities characterize how quickly charge carriers - for example electrons - move through a material when pushed by an internal electric field. The electrons in CdTe solar cells are the carriers which are responsible for the electric current generated by the

cell. By increasing electron mobility, a higher voltage and ability to produce electricity is more easily generated in the material.

However, in CdTe there seems to be a large spread of experimentally measured charge carrier drift mobilities. In large crystals of the material the drift mobilities are 1000 times greater than those measured in thin film CdTe. My project aimed to investigate why there is this large difference in measured mobilities within the same material. I measured drift mobilities in CdTe thin film solar cells using a technique called photocapacitance. Photocapacitance measures how much charge generated from the light is present in the solar cell under different internal conditions. There is a relationship between this measurement and the drift mobilities of different carriers in the cell, which I used to make my measurements.

I put my solar cell samples under a device that simulated the sun's light and measured how the photocapacitance changed as I changed the internal conditions of the solar cell. Then, once the measurement was made, I used the relationship between photocapacitance and drift mobility to determine the mobilities of different charge carriers in the sample. Most of my measurements were made on two different samples that were formed under different conditions. I was able to compare these samples at the end to find that

the charge carriers in one sample moved faster than they did in the other. This was an interesting discovery because it showed that the different conditions these materials were created under had an effect on how charges moved through them.

More important than the comparison between the two samples was the larger question of how my measurements contributed to answering why the drift mobilities were so much lower in the thin film CdTe than in single crystals. My measurements support the idea that this discrepancy is a real effect, and that the drift mobilities in thin film CdTe are extremely low. The data I obtained was not enough to truly answer why the mobilities are different, as this would require a reworking of the theory behind charge transport in these materials. However, my measurements do further support the evidence of the discrepancy, which contradicts how scientists and engineers currently model these devices. By changing how these thin film solar cells are modeled to better represent their actual properties, hopefully more effective and efficient devices can be created. This can help push solar cell technology further ahead and draw us closer to a cleaner alternative energy future.

0.2 Acknowledgements

This project is the culmination of about a year and a half of reading, work, and measurement, and could not have been possible without the help of a few important people. Firstly, I want to thank the graduate student who I spent most of my time working with, Qi Long. He taught me how to take the I-V curve and photocapacitance measurements and was always there to answer any questions I had about the experiment or to address why something might be going wrong. Without his help I would not have completed this project. Next I would like to thank my Honors Reader, Professor Matt LaHaye, for taking the time to read over various aspects of this project and provide constructive criticism and feedback. His input solidified the scientific clarity and content of my project, especially in the earlier sections. I would also like to thank the Reneé Crown Honors Program for supporting my completion of this project. Finally and most importantly, I would like to thank my research advisor Professor Eric Schiff for providing me with the opportunity to pursue a project like this and for aiding me throughout the entire process. I have learned a great deal about solar cells, solid state physics, and myself through this project, and that could not have been possible without the help and support of Professor Schiff.

0.3 Advice to Future Honors Students

For future Honors students my main piece of advice would be to start writing up your project as soon as possible. As a science student, it is hard to write up parts of your project before you have the results of your research, but you can still write up the background information beforehand. This will save you a great deal of time towards the end of your project and the end of your semester when you will be trying to summarize and interpret your results. Additionally, the less work you have to do at the end of the semester, the better. You want to be enjoying the last couple of months of your undergraduate career and not be stuck frantically writing up a Capstone project during that time.

Chapter 1

Introduction

The most active field of contemporary physics research is not astrophysics or particle physics, it is condensed matter physics. Condensed matter physics is concerned with the study of various phases of matter, primarily solids and liquids, and the physical laws and properties which describe them. The field encompasses unique phases of matter such as superconductivity and Bose-Einstein Condensation, and forms the basis of modern materials science. The multitude of material properties, such as electronic, structural, and optical properties, are measured and described by techniques founded in condensed matter physics.

One of the most important applications of materials science and condensed matter physics is in materials and technologies for alternative energy. For example, having lighter and more aerodynamic materials for wind turbine construction both reduces cost and increases the efficiency of the turbine system. My Capstone project addresses the physics of one of the most promising technologies for alternative energy, solar cells. Solar cells, also known as photovoltaic cells, are devices which convert light energy into electrical energy through the photovoltaic effect. The photovoltaic effect is the creation of a voltage or electrical current in a material due to its exposure to light. This basic principle drives solar cell technology: extracting as much energy through sunlight as possible and converting it to electricity.

There are many different types of solar cells that are in commercial use today, many of which are classified based on the type of photovoltaic material used by the cell. For example, a majority of solar cells use silicon as their primary photovoltaic material in different physical configurations, such as single junction, thin film, and multijunction cells. The single and multi-

junction solar cells refer to the number of p-n junctions in structure of the cell, where multiple junctions can produce electrical current from multiple wavelength ranges of light. These properties of semiconducting materials will be described later in the document. Thin film solar cells on the other hand, are made by depositing one or more thin layers of photovoltaic material on a substrate, the semiconductor base on which the photovoltaic material is placed. One important material used for thin film solar cells is Cadmium Telluride (CdTe), which is a crystalline compound formed from cadmium and tellurium. CdTe photovoltaic cells are the main competitors to thin film silicon technology on the commercial solar cell market today. This makes technological advances in CdTe critical to the development of thin film photovoltaic technology as a whole.

Improving the solar to electronic energy conversion efficiency is a method commonly used to increase the performance of solar cells. One way to possibly improve the efficiency is by ensuring improved voltage capabilities through higher electron drift mobilities. Drift mobilities characterize how quickly charge carriers in a material, electrons and holes, move through the material when pushed by an internal electric field. The electrons in CdTe solar cells are the carriers which are responsible for the electric current generated by the cell. By increasing electron mobility, a higher voltage and ability to produce electricity is more easily generated in the material.

However, in CdTe thin film solar cells there seems to be a large discrepancy between experimentally measured charge carrier drift mobilities. In most crystalline substances which make up solar cells, carrier mobilities are on the order of 100 $\mathrm{cm}^2/\mathrm{V}\cdot\mathrm{s}$ to 1000 $\mathrm{cm}^2/\mathrm{V}\cdot\mathrm{s}$, with silicon lying around $600 - 800$ $\mathrm{cm}^2/\mathrm{V}\cdot\mathrm{s}$. In thin film CdTe on the other hand, the range of measured drift mobilities can be three to four orders of magnitude lower than those measured in single crystals of CdTe. For example, in single crystals the drift mobility might be 800 $\mathrm{cm}^2/\mathrm{V}\cdot\mathrm{s}$ while in thin film CdTe it may be 0.08 $\mathrm{cm}^2/\mathrm{V}\cdot\mathrm{s}$. This four orders of magnitude discrepancy is showcased in Figure 1.1. My project aimed to investigate the underlying physical reasons for why these thin film mobilities differ so much from those in single crystals. This interesting physics puzzle, if solved, might lead to a better understanding of how to improve drift mobilities in thin film CdTe solar cells.

Before I began any experimentation on CdTe solar cell samples to start investigating this question, I needed to familiarize myself with the complex physics behind solar cells and drift mobilities. This required extensive reading of the scientific literature covering these complicated subjects. During the

Figure 1.1: Drift and Hall Effect mobilities for electrons and holes (charge carriers) in CdTe thin film solar cells. Note that in single crystals the mobilities are well defined while in thin films they are spread over a wide range of magnitudes.

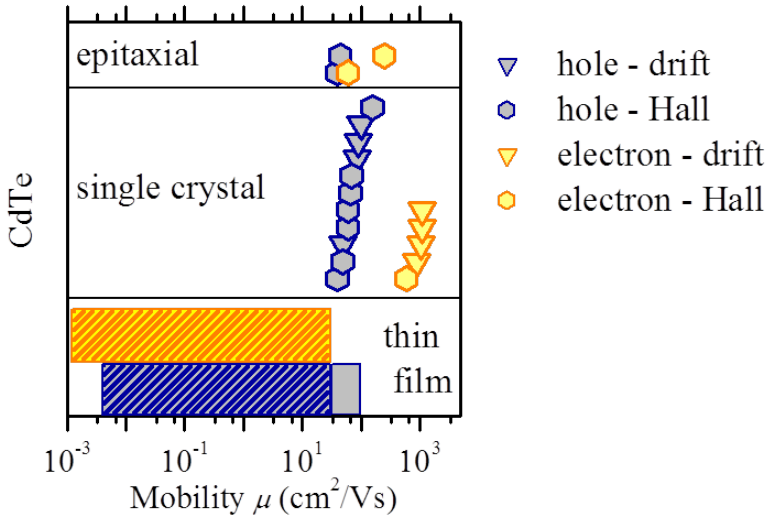

Summer of 2013 I began reading about solid state physics and semiconductor physics, which form the basic principles that solar cells utilize to operate. This investigation naturally led to a description of electronic transport phenomena and drift mobilities, which again are dependent on basic solid state physical principles, particularly effective mass theory. I then moved into solar cell device physics specifically, which focuses on the properties of the semiconducting materials and layout of the p-n junction(s) within the cell. I also read about previous drift mobility experiments performed on other types of solar cells, the different experimental techniques I would be using to acquire the necessary data, and the equipment I would be using to perform these experiments.

During the Spring semester of 2013, I began working in Professor Schiff's lab becoming familiar with the major experimental technique I would be

using to make these measurements, called photocapacitance. Photocapacitance is a quantity related to the photogenerated space charge inside the solar cell when under the influence of an applied field. If there is a large photocapacitance, the carrier mobilities will be lower (carriers are moving slower) since more carriers are grouping together in regions of space charge. Upon my return to campus in the Fall of 2013 I continued to make photocapacitance measurements on various thin film CdTe samples that the lab received from a private company called First Solar. I had been using a single lock-in amplifier setup to make my measurements, which is the standard way to measure photocapacitance. Though at one point moving to a dual lock-in amplifier setup was discussed, it was decided that the increased sensitivity and complexity of the setup was not necessary, so I stuck to the single lock-in. Instead, after many photocapacitance measurements I investigated the intensity dependence of the photocapacitance, to get a different perspective on how the mobilities were affecting the samples.

The following report begins with a summary of what I have learned about the physical description of solar cells. It begins with a chronological overview of the development of solid state physics, from the Drude Model of solids to Bloch states and effective mass theory. This theoretical basis then leads to a discussion of semiconductor physics and important ideas that arise from it such as band structure, types of semiconductors, p-n junctions, and diode behavior. From there the properties of solar cells can be described in terms of these ideas and the circuit model of a generic solar cell is presented. Next, I outline the characteristics of CdTe thin film solar cells in the context of the previously described physics. It is here that the main focus of my project comes into play: the concept of drift mobilities. Once drift mobilities are defined, the experimental method I used to find these mobilities will be explained. Finally, the results of my experiments are presented and conclusions and recommendations for future work are made.

Though the process of measuring these mobilities had its ups and downs, overall I am very proud of the work I have done and what I have accomplished. I hope that my work helps to draw attention to this very serious issue in modern thin film solar cell technology and may point scientists and researchers in the right direction toward an eventual resolution of this problem. Continued effort and resources into alternative energy research will allow us to draw ever closer to the dream of a cleaner energy future.

Chapter 2

Physical Description of Solar Cells

As stated previously, in order to gain a full understanding of the processes occurring within the solar cells and grasp the concept of what I measure when I extract mobilities from the samples, I read up on solid state physics. I began with the first models such as Drude and Sommerfeld before moving to Bloch and modern interpretations of the physics of these complicated systems. This theoretical background formed a foundation upon which I could place the semiconductor physics and solar cell device physics I would learn later and understand it better. This chapter outlines what I learned through my individual study of the subject and builds towards the description of the physics behind solar cells and their important operational parameters. The vital concept of mobilities will be addressed in a later section, building from the context constructed here.

2.1 Solid State Physics

So what is solid state physics anyway? As the name implies, solid state physics is the study of matter in the solid state, and is the largest branch of condensed matter physics. Specifically, using quantum mechanics, electromagnetism, and other physical concepts and theories, solid state physics studies how the large-scale properties of solids arise from their atomic-level characteristics. This area of physics forms the basis for modern materials science and is key to understanding how solar cells work. Before addressing

solar cells, however, it is important to understand how this subject developed, beginning with the study of metals. Metals are some of the most basic yet interesting solid structures, and they have many core characteristics. Over 2/3 of the periodic table consists of metallic elements. Metals consist of a "noble gas-like" atomic core with a small number of valence electrons, which occupy the space between the ionic cores essentially uniformly [1]. However, there is still a good amount of "empty space" in metals, resulting in a large available volume for the valence electrons to move in [1]. In order to understand metals, it is important to understand how these electrons move when in the material.

One of the first models used to describe electron transport in solids, specifically metals, was hatched by German physicist Paul Drude at the turn of the 20th Century. Drude used the idea of a classical free electron gas to construct his model, meaning that the valence electrons in the metal were free to move between the positive ionic cores without encountering any resistive forces [1]. The Drude model is classified by a few major assumptions. First of all, the scattering of an electron only occurs from a collision with an ionic core and nothing else. Next, between the collisions with the ions, the electrons do not interact with each other or other ions. These are known as the independent electron approximation and the free electron approximation respectively [1]. The collisions are assumed to be instantaneous and result in a change in the electron's velocity. Not only that, but the electron collides with a specific probability per unit time τ^{-1}, which in essence is the scattering rate. This assumption is known as the relaxation time (τ) approximation [1]. Finally, it is assumed that the only way the electrons achieve thermal equilibrium with their surroundings is through these collisions with the ionic cores of the metal.

From these assumptions it is relatively straightforward to arrive at an expression for the conductivity of the metal and its dependence on the transport properties of the electrons. The current density in the metal due to the electrons is

$$\vec{J} = -ne\vec{v} = -\frac{ne}{m_e}\vec{p} \tag{2.1}$$

where e is the electron charge, m_e is the electron mass, n is the electron number density, and $\vec{p}$ is the average electron momentum [1]. Now, we can consider the time evolution of the electron momentum subject to some arbitrary external force $\vec{f}(t)$ over some time period Δt. In this Δt the probability of a collision is $\frac{\Delta t}{\tau}$ and the probability of electrons that do not collide is

$(1 - \frac{\Delta t}{\tau})$ [1]. However, these electrons that do not collide still contribute to the average electron momentum $\vec{p}$ by an amount $\Delta\vec{p} \approx \vec{f}(t)\Delta t$. This means that the overall contribution to the average electron momentum from these electrons is

$$\vec{p}(t + \Delta t) = (1 - \frac{\Delta t}{\tau})(\vec{p}(t) + \vec{f}(t)\Delta t) \tag{2.2}$$

and taking the limit $\Delta t \to 0$ of Equation 2.2 results in

$$\frac{d\vec{p}(t)}{dt} = \frac{-\vec{p}(t)}{\tau} + \vec{f}(t) \tag{2.3}$$

[1].

The fractional damping term in Equation 2.3 is then used to derive the electrical conductivity σ. Since conductivity in metals is defined by Ohm's Law $\vec{J} = \sigma\vec{E}$ where $\vec{E}$ is the applied electric field, we need to solve for $\vec{p}(t)$, substitute it into Equation 2.1, and set that current density equal to the one from Ohm's Law [1]. To do this, we can take the external force $\vec{f}(t)$ as being that of the electric field produced by an electron in the metal $\vec{f}(t) = -e\vec{E}$ and set $\frac{d\vec{p}(t)}{dt} = 0$ to find a steady state solution for $\vec{p}(t)$ [1]. Then, by using the process described above and setting the resulting current densities $\vec{J}$ equal to each other, we arrive at the equation for electrical conductivity according to the Drude model:

$$\sigma = \frac{ne^2\tau}{m_e} \tag{2.4}$$

which results in a relaxation time $\tau \approx 1 - 10\, fs$ for a typical metal [1].

The above calculation is one of the key results of the Drude model, but unfortunately for Drude, his model has some failures. For example, it does not accurately describe and predict an important phenomena called the Hall Effect, and results in values of thermal conductivity much larger than those that are routinely measured for metals [1]. This has to do with the fact that the Drude model is a classical theory and therefore has no incorporation of quantum mechanics, which plays an important role at the atomic level of solids and undermines some of the assumptions made by the model [1]. Thankfully, after the discovery of quantum mechanics in the 1920's, a pair of German physicists named Arnold Sommerfeld and Hans Bethe modified Drude's model with the incorporation of quantum mechanics. The Sommerfeld model, as it is now known, is essentially the Drude model with the single change that the electron velocity distribution is now the quantum Fermi-Dirac distribution rather than the classical Maxwell-Boltzmann distribution

[1]. Essentially, instead of the electrons being viewed as a classical electron gas, they are viewed as a quantum electron gas.

In order to describe the Sommerfeld model it is important to introduce the notion of a concept called phase space. Phase space in quantum statistical mechanics is a space in which every possible state of a system is represented, with each possible state of the system corresponding to one unique point in the phase space [1]. The phase space describes the dynamic state of every particle in that system. For example, in quantum mechanics particles are described by wavefunctions ψ and wavevectors $\vec{k}$, so a phase space for a system may be classified by its possible wavevectors in 3-dimensional space $\vec{k} = k_x, k_y, k_z$ [1]. The phase space represented by these three wavevectors is known as k-space, and is a vital concept to solid state physics. A basic result from statistical mechanics states there may only be a certain number of states N per unit volume of phase space, where

$$N = (\frac{1}{2\pi})^j \, V_{kj} \, V_{rj} \tag{2.5}$$

and j is the number of spatial dimensions, V_{kj} is the volume in k-space, and V_{rj} is the volume in real space [1]. In the current case of electrons in solids, the number of spatial dimensions $j = 3$.

We can use the above result for the number of possible phase space states per unit volume to derive key results of the Sommerfeld model. Recall from the Drude model that we are assuming the electrons are free to move within the metal solid if the effects of the ions are ignored. In the Sommerfeld model the effects of the ions are taken into account by incorporating a constant potential $-V_0$ term into the total energy of an electron moving through the solid [1]. Through the use of quantum mechanics, we know this energy is

$$E(\vec{k}) = \frac{p^2}{2m_e} - V_0 = \frac{\hbar^2 k^2}{2m_e} - V_0 \tag{2.6}$$

since in quantum mechanics $p = \hbar k$. If we set the average potential within the metal $V_0 = 0$, then the energy is just equal to the first term of Equation 2.6, so the energy of the electrons in the solid is proportional to the magnitude squared of their wavevector $\vec{k}$ [1]. This is of critical importance, especially if we consider filling the states of k-space with different electrons at absolute zero $T = 0K$. The first electrons will occupy the lowest energy states, which correspond to the lowest wavevector magnitude of Equation 2.6 [1]. Not only

that, but each following electron is assigned to a higher energy state due to the Pauli exclusion principle, excluding any spin degeneracies.

The total number of energy states in k-space occupied by an electron is given by

$$N = 2\,(\frac{1}{2\pi})^3\,\frac{4}{3}\,\pi\,k_F^3\,V_{r3} \tag{2.7}$$

where the factor of 2 accounts for both possible spins of the electron and k_F is the radius of a k-space sphere created by the orientation of these states [1]. This radius is known as the Fermi wavevector [1]. By using Equation 2.7 to solve for k_F and recalling that the number density of electrons is $n = \frac{N}{V_{r3}}$ then we find that $k_F = (3\pi^2 n)^{1/3}$ and the corresponding electron energy is

$$E_F = \frac{\hbar^2 k_F^2}{2m_e} = \frac{\hbar^2}{2m_e}\,(3\pi^2 n)^{2/3} \tag{2.8}$$

This energy where there are no more electrons available to fill the phase space states, so the highest energy of the electrons, is known as the Fermi energy [1]. If you plug in typical values for the number density of conduction electrons in metals ($n \approx 10^{22} - 10^{23}\,cm^{-3}$) then the resulting Fermi energies correspond to the atomic energy scale ($E_F \approx 1.5 - 15\,eV$). Additionally, the velocities of electrons in the highest occupied energy states are $v_F = \frac{\hbar k_F}{m_e} \approx 0.01c$, so even in the ground state ($T = 0K$) the electrons have a large amount of kinetic energy [1].

To treat the thermal properties of electrons at temperatures higher than absolute zero we use the Fermi-Dirac distribution function from statistical mechanics, which describes how fermions occupy states as a function of their energy, and thus temperature. The Fermi-Dirac distribution has the following form:

$$f_{FD} = \frac{1}{e^{(E-\mu)/k_B T} + 1} \tag{2.9}$$

where k_B is Boltzmann's constant, μ is the chemical potential, and f_{FD} is the probability of a state of energy E being occupied by an electron [1]. The chemical potential can be defined as the amount by which a system's energy changes if a particle is added and the entropy and volume of the system are fixed. It is related to the diffusive equilibrium of the system. In terms of Equation 2.9, it is the energy at which the probability of a state being occupied is 1/2, since that would be when the denominator of f_{FD} is equal to 2. It is important to note that for this distribution, if the temperature T is

Figure 2.1: The Fermi-Dirac distribution function at $T = 0K$ (a) and at some finite temperature $T << E_F/k_B$ (b). On the x-axis ϵ represents the energy E.

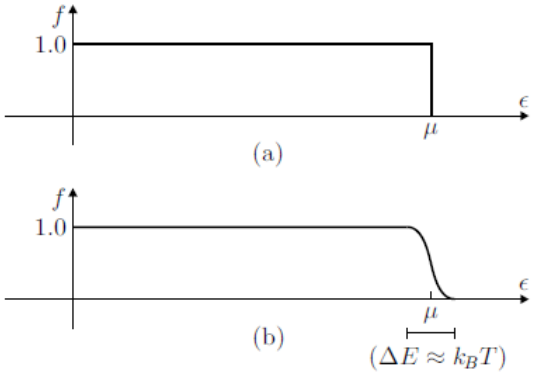

finite then f_{FD} significantly varies only within k_BT of μ, which has important consequences [1].

As the thermal energy k_BT becomes less than the Fermi energy E_F, the chemical potential μ draws closer to the Fermi energy. This means that for a typical metal at most temperatures $\mu \approx E_F \equiv \mu(T = 0K)$ [1]. Another consequence is that only electrons with energies within k_BT of the Fermi energy/chemical potential will be able to contribute to the thermal processes and transport of the material [1]. Though the Sommerfeld model successfully solved many of the thermal processes issues not addressed by Drude, it is still incomplete. The model is unable to explain the different electronic properties of solids, such as why some are insulators while others are conductors or semiconductors [1]. These problems, however, can be solved by restructuring the interactions between the ionic cores of the solid and the valence electrons. The way that solid state physicists came up with was to incorporate this interaction through a periodic potential of the crystal lattice itself in a framework known as Bloch's Theorem.

Bloch's Theorem is a formalism in quantum mechanics that is employed to deal with a periodic potential [1]. The theorem can be used to examine two opposite limits of the potential, namely a weak periodic potential where the electrons are essentially free, and a strong periodic potential where the electrons can barely move. The periodic potential $V(\vec{r})$ is introduced to embody the translational symmetry and periodicity of the crystal lattice of the solid

[1]. Essentially what this means is as you move through the crystal lattice, you see the same layout of the lattice over and over again, so it makes sense to write the potential for one part of the lattice and then simply repeat it essentially infinitely. This underlying translational periodicity is characterized in crystalline solids by what are called *primitive lattice vectors* $\vec{T}$

$$\vec{T} = n_1\vec{a_1} + n_2\vec{a_2} + n_3\vec{a_3} \tag{2.10}$$

where n_1, n_2, n_3 are integers and the $\vec{a}$ vectors are not in the same plane [1].

Since the potential $V(\vec{r})$ is periodic, it follows that $V(\vec{r}) = V(\vec{r}+\vec{T})$. The existence of periodicity also implies that the potential can be represented as a Fourier series

$$V(\vec{r}) = \sum_{\vec{G}} V_G\, e^{i\,\vec{G}\cdot\vec{r}} \tag{2.11}$$

where $\vec{G}$ are a set of vectors and V_G are the Fourier coefficients [1]. Both of the above conditions of periodicity have further implications, namely that $e^{i\,\vec{G}\cdot\vec{T}} = 1$ and therefore $\vec{G}\cdot\vec{T} = 2p\pi$ where p is some integer. This means that we can find the set of vectors $\vec{G}$

$$\vec{G} = m_1\vec{A_1} + m_2\vec{A_2} + m_3\vec{A_3} \tag{2.12}$$

where the m's are again integers and the $\vec{A}$ vectors are not coplanar and defined by $\vec{a}_j\vec{A}_l = 2\pi\delta_{jl}$ where δ_{jl} is the Kronecker delta [6]. The Kronecker delta is 1 when the indices j and l are equal and is 0 for all other values of j and l. The above equations for the sets of vectors $\vec{T}$ and $\vec{G}$ show that the existence of a lattice in real space (from the $\vec{T}$ vectors) automatically implies the existence of a lattice in k-space (from the $\vec{G}$ vectors). As a result, the $\vec{G}$ vectors define what is known as the *reciprocal lattice* with primitive translation vectors $\vec{A_j}$ [1]. The idea of a reciprocal lattice is vital to solid state physics and has important consequences. For example, instead of dealing with the energy relationship for one electron $E(\vec{k})$ there must be an infinite number of equivalent relationships such that for all $\vec{G}$, $E(\vec{k}) = E(\vec{k}+\vec{G})$ [1].

Now that the basic lattice characteristics and results of periodicity have been defined, we must find functions that can describe the motions of electrons through the periodic lattice potential which also reflect the periodicity of the lattice. To obtain these functions, the correct wavefunctions to describe the electrons, we must solve the time-independent schrödinger equation for the periodic potential we have constructed [1]. The process of solving the

equation is not as important as the result, which is given by Bloch's Theorem. Bloch's Theorem states that the eigenstates (eigenfunctions ψ) of a one electron Hamiltonian $H = -\frac{\hbar^2\nabla^2}{2m} + V(\vec{r})$ with a periodic potential $V(\vec{r}) = V(\vec{r}+\vec{T})$ have the form of a plane wave times a function U with the periodicity of the lattice

$$\psi_q(\vec{r}) = e^{i\,\vec{q}\cdot\vec{r}}\,U_{j,\vec{q}} \tag{2.13}$$

where $\vec{q} = \vec{k} - \vec{G}$ [1]. The eigenstate wavefunctions ψ_q are known as the Bloch wavefunctions. This theorem is true for any particle propagating in a periodic lattice, not just electrons, and makes no assumptions about the overall strength of the potential [1].

Bloch's Theorem has introduced the wavevectors $\vec{q}$ and $\vec{k}$, which looks similar to the $\vec{k}$ we saw from the quantum mechanics in the Sommerfeld model where $\vec{p} = \hbar\vec{k}$. However, the wavevector $\vec{k}$ from Bloch's Theorem is not an eigenstate of the momentum operator [1]. In other words, it has nothing to do with the momentum of the particle being described by the Bloch wavefunctions. Instead, the value $\hbar\vec{k}$ in this context is called the *crystal momentum*, which is the momentum of the system as a whole. In essence, $\vec{k}$ can be thought of as a quantum number (called the *crystal wavevector*) which describes a certain Bloch wavefunction state, and thus a state of the system [1]. What is interesting about these Bloch states is that they will continue to exist forever in an infinite and periodic crystal. The electrons described by these states will not scatter off of anything in the crystal unless there is disorder in the lattice (disturbs perfect periodicity) or they encounter boundaries (destroys infiniteness/periodicity) [1]. In essence this result is a byproduct of the wave-like nature of electrons, as a wave can propagate indefinitely in a periodic array of potential scattering sites due to the coherent constructive interference of any scattered waves [1].

The crystal wavevector $\vec{k}$ is vital to understanding the bandstructure of solids, a key concept of solid state physics. The bandstructure of a solid usually refers specifically to its electronic dispersion $E(\vec{k})$, or how the energy of an electron in the solid varies as a function of the crystal wavevector [1]. We remember from the Sommerfeld model that the dispersion of a free electron is simply the first term in Equation 2.6, $\frac{\hbar^2k^2}{2m}$. Since this equation has no dependence on the direction of $\vec{k}$ and only on the magnitude k it is said to be isotropic. As a result, the Sommerfeld model produces this same parabolic bandstructure regardless of the material [1]. This does not reflect reality however, where the bandstructure/dispersion of the material changes dras-

tically over small energy ranges or small differences in k. In order to more accurately describe bandstructure it is useful to derive a quantity called the effective mass, which helps parameterize the electrons in each band (each unique dispersion value, changes with k) when they are subject to an external force [6].

To derive the effective mass, let us exert an external force f in one dimension on a band electron, so one moving in a lattice with a unique dispersion. This external force will perform an amount of work on the electron equal to $\Delta E = fv\Delta t$ in some time Δt [6]. However, the force will also perform work on the lattice itself equal to

$$\Delta E = \frac{dE}{dk}\Delta k = \hbar v \Delta k \tag{2.14}$$

from the dispersion of a free electron. Setting these two equations for the work done equal to each other and solving for the external force f, we find that in the limit $\Delta t \to 0$, $f = \hbar \frac{dk}{dt}$ [6]. In three dimensions, this result easily generalizes to

$$\vec{f} = \hbar \frac{d\vec{k}}{dt} \tag{2.15}$$

which is the external force felt by an electron in a crystal lattice.

Now, we can calculate the rate of change of the velocity of the electron with time by

$$\frac{dv}{dt} = \frac{1}{\hbar}\frac{d^2E}{dkdt} = \frac{1}{\hbar}\frac{d^2E}{dk^2}\frac{dk}{dt} \tag{2.16}$$

[6]. Using the result from Equation 2.15 we can substitute $f/\hbar$ for $\frac{dk}{dt}$ and solve for the external force to get

$$\frac{\hbar^2}{\frac{d^2E}{dk^2}}\frac{dv}{dt} = m^*\frac{dv}{dt} = m^* a = f \tag{2.17}$$

where the effective mass m^* is defined by

$$m^* = \frac{\hbar^2}{\frac{d^2E}{dk^2}} \tag{2.18}$$

[6]. The effective mass gives a convenient way of describing the motion of band electrons subject to an external force, as seen in Equation 2.17 where the external force f can be expressed as Newton's Second Law $f = ma$ with

the effective mass substituted for the inertial mass [6]. In general the effective mass is a quantity which is energy-dependent and can be either positive or negative, in contrast to the inertial mass which is uniquely positive. The effective mass is important in terms of defining the carrier drift mobility in semiconductors, but more on that later.

2.1.1 The Physics of Semiconductors

Solids are classified electrically into three main categories: conductors, semiconductors, and insulators. Each of these categories represents the material's ability to conduct, partially conduct, or not conduct electricity, respectively. Most metals are classified as conductors since electrons flow within them quite easily, while some solids are insulators and do not generate electronic current at all [1]. Solar cells fall under the interesting category of semiconductors. Semiconductors have an electrical conductivity between that of insulators and conductors, which can be changed by the addition of other substances into the semiconductor. Regardless of classification, all of these solids adhere to the electronic bandstructure model that was previously discussed, formed from the Bloch states and dispersion relations of the electrons in the solid [1]. These bands form allowed and forbidden energy ranges for electrons in the solid, and it is these ranges or bands which end up determining the electrical classification of the material [6].

The electronic bands in solids contain either allowed states or forbidden states for electrons as a result of quantum mechanics. Quantum mechanics requires that the atoms in the crystal lattice have discrete energy levels rather than a continuum, meaning there are only specific energy states that electrons can occupy [1]. As a result, there end up being gaps between allowed energy bands, called band gaps. Though there are many band gaps throughout the electronic structure of a solid, the most important and commonly referred to band gap is the one between two specific bands called the *valence band* and the *conduction band* [6]. The *valence band* is the highest range of electron energies in which electrons are normally present at $T = 0K$, or absolute zero. The electrons present in this band are called valence electrons, and are bound to individual atoms as opposed to moving freely within the atomic lattice. On the other hand, the *conduction band* is the range of electron energies high enough to free an electron from its binding atom and allow it to move freely within the atomic lattice as a "delocalized" electron [6]. The electrons present in the conduction band are called conduction elec-

Figure 2.2: A diagram representing the electronic band structure in solids. Insulators are characterized by large band gaps, semiconductors by small band gaps, and conductors by no band gap (overlapping bands). The conduction band is in blue and the valence band is in red.

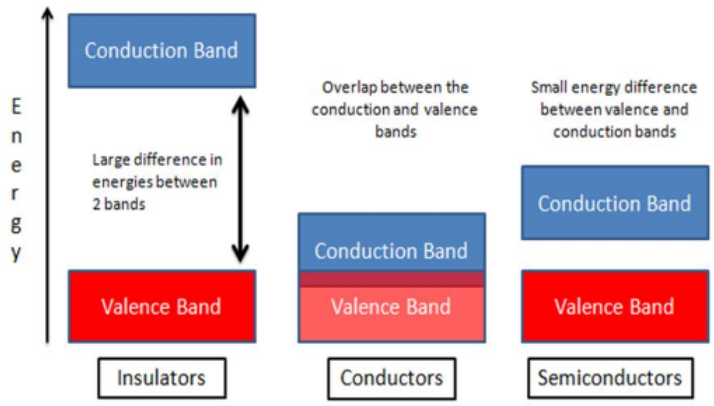

trons and are the charge carriers of the material: they are responsible for the conduction of electricity in the material.

The band gap is the energy range in the solid containing forbidden electron states, specifically the energy difference between the top of the valence band and the bottom of the conduction band. The energy range of the band gap is important because it is equivalent to the energy necessary to free a valence electron from its binding atom and allow it to move freely within the solid in the conduction band [6]. This is a critical factor in determining the conductivity of a solid. Materials with large band gaps tend to be insulators, while those with little to no band gap tend to be conductors, as shown in Figure 2.2. Semiconductors are classified by a small but nonzero band gap, which allows thermal vibrations and excitations to excite electrons across the band gap into the conduction band [6].

There are three different types of semiconductors, classified by the nature of the impurities present in the semiconductor: i-type, p-type, and n-type. Intrinsic or i-type semiconductors are pure semiconductors without any dopant materials present [6]. A dopant is an impurity element that is inserted into a substance in very low concentrations in order to alter the electrical proper-

ties of the material. When a dopant is added to a semiconductor it usually takes the place of elements that were in the lattice of the solid, and ends up altering the Fermi level of the semiconductor [6]. The Fermi level is simply the Fermi energy from Equation 2.8 we found in the Sommerfeld model. In semiconductors the Fermi level or Fermi energy is important, as changing it slightly through the addition of a dopant (doping) results in a material with mainly positive or negative primary charge carriers. This is where the other types of semiconductors come in, as p-type semiconductors have predominantly positive charge carriers from doping and n-type semiconductors have mainly negative charge carriers [6]. Intrinsic semiconductors have the proportions of their charge carriers determined by the original properties of the semiconducting material rather than by the impurities introduced through doping.

But what are positive charge carriers if electrons are the negative charge carriers? The answer is that in fact, the absence of an electron acts as a net positive charge carrier called a *hole*. A hole is, in essence, the absence of an electron from an otherwise relatively full valence band. For example, as previously stated, the band gaps of semiconductors are small enough that small thermal excitations are energetic enough to excite an electron across the band gap from the valence band to the conduction band [6]. This leaves behind a net positive charge in the valence band from the absence of the electron called a hole, which acts as a positively charged particle. It carries a positive electric charge and responds to electric and magnetic fields as if it had positive charge and mass [6]. The effective positive mass holes have is actually attributed to a negative electron effective mass, in that $m_h^* = -m_e^*$ where m_h^* is the effective mass of the hole [6]. Electrons and holes, the charge carriers in semiconductors, have a unique relationship with each other characterized by generation and recombination. Carrier generation occurs when electrons gain energy and move from the valence band to the conduction band, producing what is known as an electron-hole pair. The pair may either separate into two mobile charge carriers or recombine, where the conduction band electron loses energy and re-occupies the energy state of the hole in the valence band [6].

P-N Junctions & Diodes

The interaction between electrons and holes is vital to understanding how semiconductors are used in modern electronics, including solar cells. It is

Figure 2.3: A p-n junction at zero bias. The carrier concentrations of holes and electrons overlap in the space charge or depletion region, which has an electric field that acts in opposition to the carrier diffusion.

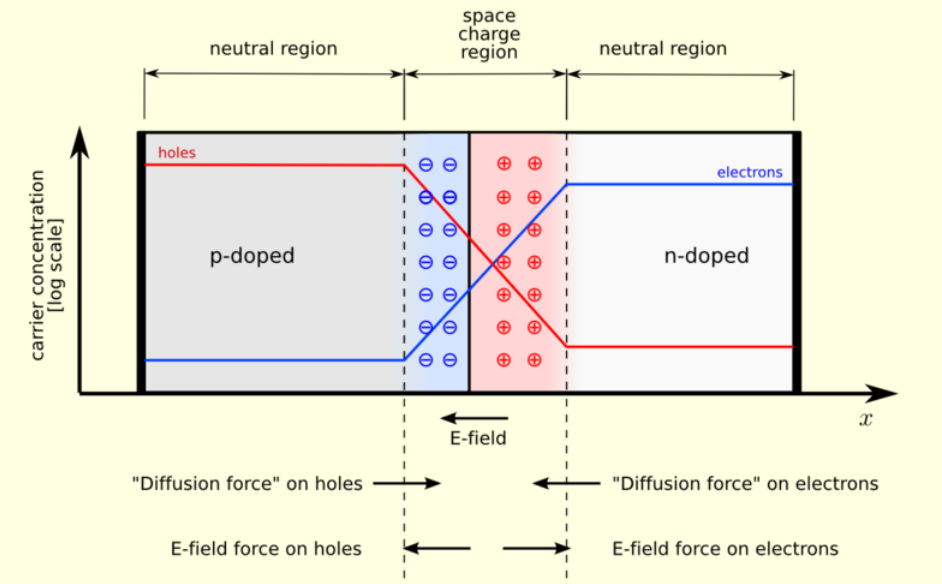

now clear that if n-type semiconductors produce more negative charge carriers then they generate more electrons, and therefore p-type semiconductors have an abundance of holes. Modern electronics technology is hinged upon the merging of these two types of semiconductors in a *p-n junction*. A p-n junction is a boundary or interface between p-type and n-type semiconductor materials inside a single crystal of a semiconductor created by doping [6]. The p-n junction is where the electronic action of the semiconductor takes place, due to the concentration gradient of the interface between the n and p type semiconductors. Since there is a high concentration of electrons on the n-type side and a low electron concentration on the p-type side, the electrons will diffuse from the n region to the p region [6]. This will leave behind positively charged holes in the n region close to the interface and build up a negative charge in the p region from the electron diffusion. The reverse of this process occurs for holes, where they diffuse from the p side to the n side of the junction, leaving negative charges behind and generating positive charges on the n side [6].

Originally the p-type and n-type semiconductors are electrically neutral

even though they have large carrier concentrations, but the diffusive action across the interface results in a loss of neutrality and the regions closest to the interface become charged [6]. The charge build-up in this region, known as the space charge or depletion region, creates an electric field from the positively charged n region to the negatively charged p region. This electric field counteracts the diffusion of carriers across the interface, pushing them back to their respective regions. So while electron and hole diffusion would generate a greater depletion region, the electric field of the region itself acts against the diffusion [6]. Eventually the electric field will be strong enough to counteract any further diffusion and the junction will come to diffusive equilibrium.

When this happens the space charge region actually contains no mobile charge carriers, just the overall net doping level of the interface [6]. This explains why the region is usually called the *depletion region*, the region which is fully depleted of charge carriers upon reaching diffusive equilibrium, meaning it acts as an insulator. The p-n junction in semiconductors is used as the basis of most modern electronics through the process of controlling the depletion region. By applying a *bias* (applied voltage) to the p-n junction, one can control the direction of carrier diffusion and the strength of the electric field in the depletion region [6]. For example, by applying the right bias voltage the diffusion of electrons could increase dramatically, generating electrical current that flows throughout the semiconductor. This concept forms the basis of diode behavior, one that is critical to the operation of solar cells.

A diode is a two terminal electronic component which has an inverse relationship between directions of current flow: it has low resistance to current flow in one direction and high resistance to current flow in the other direction [6]. Electronic terminals are points where a conductor from an electrical component or device comes to an end and provides a point of connection to external circuits. A semiconductor diode is a piece of semiconductor material with a p-n junction connected to two electronic terminals. The main function of any diode is to allow electric current to pass in one direction, known as the *forward* or *forward biased* direction, while blocking current in the opposite direction, the *reverse biased* direction [6]. This type of behavior, where current is only allowed to flow in one direction, is called *rectification* and is used in modern electronics to convert alternating current electricity to direct current electricity.

In semiconductor diodes, the n-type side of the p-n junction is called the cathode and the p-type side is called the anode. The diode allows electrons to

flow from the cathode to the anode, but not in the reverse direction. Another key characteristic of semiconductor diodes is that they only begin conducting electricity if a certain threshold voltage is present in the forward direction [6]. In this case of forward bias, a positive voltage is applied across the p-n junction, with the p-type side at the positive terminal and the n-type side at the negative terminal. The positive potential on the p side repels the holes, while the negative potential on the n side repels the electrons [6]. When the electrons and holes are pushed toward the junction, the distance between them decreases. As the forward-bias voltage increases, the depletion region eventually becomes thin enough that its electric field cannot counteract charge carrier motion across the p-n junction, so the carriers begin to move with lower resistance in that direction [6]. If the external applied voltage is in the same direction (same polarity) as the internal electric field of the p-n junction, in this case reverse biased, then the depletion region will continue to act as an insulator that inhibits significant current flow in that direction.

A special type of diode used in the design of solar cells is called a photodiode, which is a type of photodetector that can convert light into electrical current or voltage [6]. Photodiodes are designed to operate in reverse bias, where the voltage at the cathode is higher than the voltage at the anode. In the case of a semiconductor p-n junction diode, this means the applied voltage is larger at the n-type side and smaller at the p-type side of the junction. The special characteristic of photodiodes is their utilization of the photoelectric effect. If an incident photon has enough energy when it strikes the diode it excites an electron, creating a free electron and a hole, an electron-hole pair [6]. If the photon is absorbed in the depletion region of the p-n junction, the generated charge carriers are moved from the junction by the built-in electric field so that the holes move to the anode and the electrons move to the cathode, generating a photocurrent [6].

There is a specific type of diode used in many solar cells called a pin diode. Pin diodes have a wide, lightly doped, nearly intrinsic or i-type semiconductor region in between the n-type and p-type regions of the semiconductor [6]. This makes them worse rectifiers, but better photodetectors, as the large intrinsic region allows the internal electric field of the depletion region to extend further into the material. This helps to speed up the transport of charge carriers across the depletion region and results in faster overall operation of the diode [6]. As a photodetector or photodiode the pin diode operates in reverse bias, where the photon entering the intrinsic region again frees a charge carrier and the reverse bias field creates the photocurrent. This type

of structure is important in solar cells because it results in a better response of the device for long-wavelength photons which penetrate more deeply into the cell. Since only electron-hole pairs generated in the depletion region contribute to the photocurrent, the larger depletion region in a pin diode due to the intrinsic region enables greater current generation throughout a larger device volume [6].

2.2 Solar Cell Device Physics

Now we have finally constructed the theoretical framework with which we can use to tackle the physical background of how solar cells operate. Specifically, we want to describe the processes by which light is converted to electrical current when striking a suitable semiconductor lattice [3]. This process starts when a photon strikes the semiconductor material that makes up the solar cell, where one of three things can happen. The photon could pass straight through the material of the solar cell if it has low enough energy and a correspondingly long wavelength, or it could simply reflect off of the surface of the cell [3]. The third possibility is the most exciting and interesting, as a photon can be absorbed by the material if its energy is higher than the band gap of the semiconductor, generating an electron-hole pair. If the photon has an energy much higher than the band gap of the material, the excess energy is converted to heat and increases the overall temperature of the material, rather than usable electrical current from further electron-hole pair generation [3]. There are some solar cells, however, which utilize special properties of the material itself to absorb one photon and create multiple electron-hole pairs. This unique process is known as multi-exciton generation and is a current area of solar cell technology and materials research [4].

As we know from the previous discussion of the physics of semiconductors and diodes, if the incident photon's energy is higher than the band gap then an electron from the valence band is excited into the conduction band where it can freely move throughout the material, along with leaving behind a positively charged hole [3]. Interestingly enough, holes themselves don't actually move. The valence electrons around them move to fill the empty space the hole has left, effectively moving the hole throughout the valence band of the material's lattice [3]. Though this is one way charge carriers move in solar cells, there are two main processes which drive the motion of the charge carriers: drift and diffusion. Drift is essentially movement caused

Figure 2.4: A representation of the circuit model of a solar cell where I_{photo} is the photocurrent, I_D is the photodiode current, V_D is the voltage across the photodiode, I is the output current, V is the voltage across the output terminals, and R_{sh} and R_s are the shunt and series resistances respectively [3].

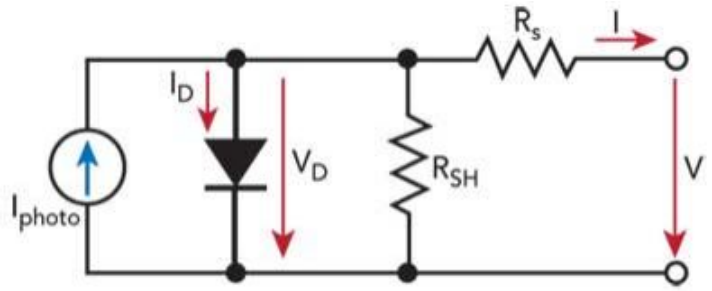

by an electric field applied across the solar cell, which can be an externally or internally driven field [3]. Diffusion is movement due to the random thermal motion of the charge carriers, which occurs in between the edges of the depletion region, where the electric field takes over. It is important to note that in thin film solar cells the dominant method of charge carrier movement is drift, caused by the electric field of the internal p-n junction [3].

Solar cells are especially interesting to describe physically because they can be modelled by an equivalent electronic circuit. An ideal solar cell can be represented by a current source in parallel with a photodiode, though since in practice no solar cell is ideal, two resistances are added to the model [3]. These two resistances are called the shunt and series resistances, represented by R_{sh} and R_s respectively. The series resistance arises from the fact that the solar cell is not a perfect conductor of electricity, and the shunt resistance is caused by a leakage of current between the two output terminals [3].

The overall current produced by the solar cell, which passes through the series resistor in the equivalent circuit (Figure 2.4), is given by the following equation:

$$I = I_{ph} - I_D - I_{sh} \tag{2.19}$$

where I_{ph} is the photocurrent generated by the solar cell, I_D is the current through the photodiode (usually small), and I_{sh} is the current through the shunt resistor. The voltage relationship for the elements of the circuit, which

governs the total current through Ohm's Law $V = IR$, is given by

$$V_D = V + IR_S \tag{2.20}$$

since the voltage across circuit components in parallel is equivalent. The current through the diode, I_D is governed by the characteristic equation for current through a diode

$$I_D = I_0 \, (e^{\frac{q \, V_D}{n \, k_B \, T}} - 1) \tag{2.21}$$

where I_0 is the reverse saturation current, q is the unit of elementary charge, k_B is Boltzmann's constant, T is the temperature in Kelvin, and n is the diode ideality factor, which equals one for an ideal diode [3].

These specific parameters for the current behavior of a diode are important to the overall performance of the solar cell, as it essentially acts as a photodiode due to the action of the p-n junction. In order to finish the equation for the overall current output of the solar cell, we can calculate the shunt current I_{sh} from Ohm's Law: $I_{sh} = \frac{V_D}{R_{sh}}$. Finally, substituting this equation, Equation 2.20, and Equation 2.21 into Equation 2.19 yields the *characteristic equation* of a solar cell, which relates key solar cell parameters to the output current and voltage [3]

$$I = I_{ph} - I_0[exp(\frac{q \, (V + IR_s)}{n \, k_B \, T}) - 1] - \frac{V + IR_s}{R_{sh}} \tag{2.22}$$

The most common useage of this characteristic equation is using nonlinear fitting methods to extract the values of the parameters I_0, n, R_s and R_{sh}, since they can't be measured directly [3]. These parameters describe the overall nonlinear model of how electricity flows in solar cells. However, these parameters do not characterize the overall performance of the solar cell in terms of its operation and ability to convert light to electricity.

2.2.1 Basic Solar Cell Parameters

The four parameters that are most often used to characterize the performance of solar cells are the short circuit current I_{sc}, the open circuit voltage V_{oc}, the fill factor FF, and the efficiency η [3]. It is these parameters which are most often seen together when describing a solar cell and its solar to electric energy conversion capabilities. The short circuit current I_{sc} is the

current when the output terminals of the solar cell are connected to each other, resulting in the corresponding voltage across the solar cell $V = 0$ [3]. The short circuit current is produced by the creation and collection of light-generated charge carriers, which for an ideal solar cell is approximately equal to the photocurrent produced by the cell $I_{sc} \approx I_{photo}$. In this sense, I_{sc} is the largest current that can be extracted from the solar cell [3]. Though I_{sc} is dependent on the area of the solar cell, to compare cells of different areas the short circuit current density J_{sc} is usually used, where the short circuit current is divided by the area of the solar cell $J_{sc} = \frac{I_{sc}}{A}$. Additionally, I_{sc} is dependent on the optical properties and charge carrier collection properties of the solar cell, as well as the overall spectrum and intensity of the incident light [3].

Next is the open circuit voltage V_{oc}, which is equivalent to the voltage between the output terminals when no current is flowing through the solar cell $I = 0$. This is also equivalent to the maximum voltage available for the solar cell, and corresponds to the amount of forward bias (positive voltage) on the solar cell due to the bias of the internal p-n junction from the generated photocurrent [3]. The open circuit voltage can be found by setting Equation 2.22 equal to 0 and solving for the voltage V. If the shunt resistance R_{sh} is large enough, the final term of the characteristic equation can be neglected, resulting in

$$V_{oc} = \frac{n\, k_B\, T}{q} \ln(\frac{I_{photo}}{I_0} + 1) \tag{2.23}$$

[3]. Though this equation for V_{oc} depends on some of the intrinsic diode parameters, the open circuit voltage may also be dependent on the charge carrier concentrations in the solar cell.

The fill factor FF is a quantity used in conjunction with V_{oc} and I_{sc}/J_{sc} to determine the maximum power that can be delivered by a solar cell. It is defined as the ratio of the maximum power from the solar cell to the product of V_{oc} and I_{sc}

$$FF = \frac{V_{mp} I_{mp}}{V_{oc} I_{sc}} \tag{2.24}$$

where V_{mp} and I_{mp} are the voltage and current produced at maximum power, respectively [3]. The fill factor essentially gives a measure of how much of the V_{oc} and I_{sc} is utilized when the solar cell is delivering its maximum power. The value of the fill factor is directly related to the values of the series and shunt resistances, as both R_{sh} and R_s would have negative effects on I_{sc} and

V_{oc} [3]. Typical fill factors for commercial solar cells are around or greater than 0.70.

The most common parameter used to compare and evaluate the performance of solar cells is the efficiency η. The efficiency of a solar cell is defined as the ratio of the the electrical energy output from the solar cell to the energy input the solar cell receives from the sun [3]. Essentially, this represents the percentage of the sun's energy over the area of the solar cell that is converted in to electrical energy and power. The solar cell efficiency is calculated by taking the ratio of the solar cell's maximum power output to the power input from the incident sunlight:

$$\eta = \frac{P_{max}}{P_{in}} = \frac{V_{oc} I_{sc} FF}{P_{in}} \tag{2.25}$$

where P_{max} follows from Equation 2.24 [3]. The input power from the incident sunlight P_{in} is measured in watts per square meter (W/m^2) and for standard efficiency calculations is usually taken to be 1 kW/m^2. There are many factors which affect and influence a solar cell's conversion efficiency, namely the spectrum and intensity of the incident sunlight, the efficiency of charge carrier separation in the p-n junction of the solar cell, and the temperature of the solar cell [3]. The efficiency η even has a maximum theoretically possible value given by the Carnot limit, the upper limit of the efficiency of most thermodynamic systems, which for solar cells is around 86% for the temperature of photons emitted by the sun [3]. Incident photons with an energy lower than the band gap are converted to heat if they are absorbed by the cell, further lowering the thermodynamic limit to η. The combination of these four key solar cell parameters, I_{sc}, V_{oc}, FF and η provide a complete description of the performance of the solar cell.

Chapter 3

Cadmium Telluride & Mobilities

Equipped with the solid state and semiconductor physics background, as well as the detailed description of how solar cells work and the parameters associated with them, we can now begin looking specifically at Cadmium Telluride (CdTe) solar cells. The structure and description of CdTe thin film solar cells is outlayed in this section, as well as a physical description of drift mobilites and their importance to understanding and improving solar cell technology.

3.1 Cadmium Telluride Solar Cells

We know from the introduction to this report that thin film solar cells are cells made by depositing one or more thin layers of photovoltaic material on a substrate, the semiconductor base on which the photovoltaic material is placed. This lowers the overall cost of the solar cell, as the thin film uses less of the expensive semiconductor material. Specifically, thin film CdTe solar cells require ≈1-2% of the semiconductor material needed by traditional silicon solar cells [4]. Cadmium telluride thin film technology is also the only type of thin film solar cell to be cheaper than crystalline silicon for a majority of the photovoltaics market. With any solar cell, the type of solar cell (silicon, CdTe, etc.) denotes specifically the absorber layer of the solar cell, responsible for the absorption of incident photons and generated photocurrent by the cell [4].

In general solar cells consist of the substrate, one or more transparent conducting films, a window layer, the absorber layer, and a metallic back contact (see Figure 3.1) [4]. As stated previously, the substrate is the material on which everything else is deposited, which in the case of CdTe is usually glass. Transparent conducting films (TCFs) are thin layers of optically transparent and electrically conductive materials [4]. Optically transparent refers to a quality of the material that allows photons to pass directly through the material without being scattered. TCFs themselves usually act as windows for light to pass through to the materials beneath where carrier generation occurs or as contacts for unwanted carriers to transport out of the solar cell [4]. These TCF materials typically have band gaps corresponding to the range of visible wavelengths of light in the electromagnetic spectrum, meaning photons with energies below this band gap cannot pass through the TCF and only visible light passes through [4]. Some typical inorganic TCFs are the transparent conducting oxides indium-tin-oxide (ITO) and zinc oxide (ZnO).

In thin film and single-junction solar cells, window layers are the top layers that are made of high band gap materials, which allow the transmittance of sunlight to the layers afterwards [4]. Though these may serve a similar purpose to the TCF layers, TCF layers may be used for other purposes, while the window layer adheres to its description. The metallic contact on the back acts as a conductor, which can pick up the photogenerated electrons and carry the current out of the solar cell [4]. Then comes the most important layer and where CdTe comes into play - the absorber layer. Again as stated previously, the absorber layer of the solar cell is responsible for the absorption of incident photons and generated photocurrent by the cell. Cadmium telluride has a band gap that is almost optimally matched to the solar spectrum of photons for photovoltaic energy conversion [4]. CdTe has a band gap of $1.5eV$ where eV stands for electron-volt, a unit of energy corresponding to the amount of energy gained or lost by a single electron moving across an electric potential difference of one volt. This band gap value, coupled with a high absorption coefficient for CdTe (greater ability to absorb incident photons), results in the ability for CdTe to absorb photons over a wide wavelength range [4]. CdTe can absorb photons from the ultraviolet range of the spectrum to the bandgap at the edge of the visible spectrum at around $825nm$ [4].

The most common layout of a CdTe thin film solar cell is as follows. First, the glass substrate is coated with a TCF, usually ITO. Next comes the window layer, which is usually Cadmium Sulfide (CdS) [4]. However, to obtain

Figure 3.1: A possible configuration of materials in a CdTe thin film solar cell. TCO stands for transparent conducting oxide, a typical TCF for thin film solar cells.

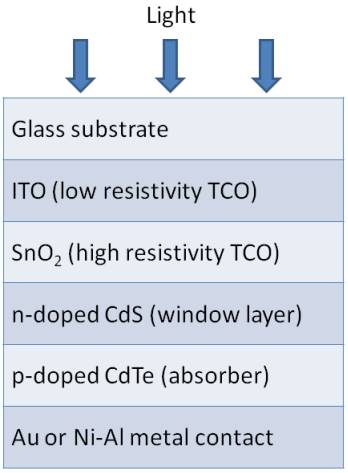

a high current density (current per unit area) in the solar cell the CdS layer needs to be as thin as possible. This is so that a large number of photons with energies greater than the band gap of CdS can reach the CdTe absorber layer beneath and generate photocurrent [4]. The CdS window layer is also usually doped so that it becomes an n-type semiconductor, and correspondingly the CdTe absorber layer is doped to become a p-type semiconductor. This causes the main photodiode p-n junction of the cell to occur between the n-type CdS window layer and the p-type CdTe absorber layer [4]. This type of solar cell configuration is shown in Figure 3.1.

3.2 Mobilities and Their Importance

My Capstone project is concerned with charge carrier transport within CdTe solar cells, specifically the carrier mobilities. In intrinsic semiconductors, we know that free electrons are created from thermal excitations of the atoms in the valence band of the material, ionizing them [6]. The free electrons can then move around in the crystal lattice as conduction electrons or recombine with the positive ions, namely the hole left by their disappearance. At thermal equilibrium, the ionization rate of the atoms in the lattice is equivalent

to the recombination rate of the generated electron-hole pairs [6]. This means that unless there is some applied external force, namely an electric field or a charge gradient in the material, any freed electrons will undergo a negligible net displacement due to the equivalent generation and recombination rates at thermal equilibrium. A negligible displacement of electrons results in a negligible current within the material, which is clearly not ideal for a solar cell. However, the built-in field created by the p-n junction in a solar cell provides an avenue to avoid the problem posed by thermal equilibrium.

Recall from the Drude model that free electrons are assumed to move around freely in a static lattice of positive ions [1]. This is a good approximation for conditions at thermal equilibrium. Now, say a free electron is being acted on by the built-in electric field of the p-n junction of the solar cell. When the $\vec{E}$ field is applied to the electron, it is accelerated in the direction of the field until it undergoes a collision with other electrons or the ions in the lattice [1]. The average distance the electron moves before it collides with another electron or lattice ion is known as the *mean free path length* or *drift length*. During the mean free path, the momentum applied to the electron is given by the force due to the applied electric field (eE) and the lifetime of the free electrons τ_e: $p = \frac{eE}{\tau_e}$ where e is the electron charge and E is the magnitude of the applied field [6]. The momentum gained by the electron during this motion is given by the usual equation for momentum, but using the effective mass instead of the inertial mass and the drift velocity of the electron in the lattice: $p = m_e^* v_e$ [6]. Due to conservation of momentum, these momenta must be equivalent, and solving for the drift velocity results in

$$v_e = (\frac{e\tau_e}{m_e^*})E \tag{3.1}$$

The result from Equation 3.1 states that the drift velocity of a free electron in the semiconductor lattice is proportional to the applied electric field. The proportionality factor between the applied field and the drift velocity is in fact the *electron drift mobility* μ_e,

$$\mu_e = \frac{e\tau_e}{m_e^*} \tag{3.2}$$

[6]. A similar expression can be used for holes, simply by flipping the charge and changing the lifetime and effective mass to that of a hole moving through

the lattice

$$\mu_h = -\frac{e\tau_h}{m_h^*} \tag{3.3}$$

[6]. The electron and hole drift mobilities are defined as the drift velocity of the respective charge carrier (electron or hole) per unit electric field, where the lifetimes are for electrons in the conduction band and holes in the valence band [6].

The drift mobilities are measured in units of $\mathrm{cm}^2/\mathrm{V}\cdot\mathrm{s}$ and are directly related to the mean free time between collisions, namely the scattering rate, given by the reciprocal of the carrier lifetime

$$electron\,scattering\,rate = \frac{1}{\tau_e} \tag{3.4}$$

$$hole\,scattering\,rate = \frac{1}{\tau_h} \tag{3.5}$$

[6]. This scattering rate is determined by various mechanisms within the structure of the material, where the two most dominant mechanisms are lattice scattering and impurity scattering. Lattice scattering results from thermal vibrations of the atoms in the crystal lattice at any temperature above absolute zero [6]. These vibrations disturb the periodic potential of the lattice and allow energy to be transferred between the charge carriers and the lattice itself [6]. The rate and magnitude of the thermal vibrations increases with temperature, resulting in increased scattering due to the lattice vibrations and a decreased carrier lifetime, both of which lead to lower drift mobilities. Impurity scattering results when a charge carrier travels past an ionized dopant impurity, seen as a defect in the crystal structure [6]. The trajectory of the charge carrier is then altered due to the Coulomb force interaction between the charged bodies. The probability of this type of scattering depends on the overall concentration of ionized impurities in the material, and the scattering rate decreases with increasing temperature [6].

Regardless of the scattering mechanism, charge carrier mobilities are important in determining the electrical properties of solar cells. High mobilities result in more effective charge collection and photocurrent generation, since charges move across cell area and into the back contact more easily. Slower mobilities mean increased scattering and decreased photocurrent, which can negatively impact the overall performance of the solar cell. Understanding how to improve the performance of low mobility solar cells would be a large step forward in the development of solar cell technology.

Chapter 4

Experiments

In order to measure the charge carrier drift mobilities in various CdTe solar cell samples, I used a technique called photocapacitance. This technique was previously used in amorphous silicon solar cells to address an issue where the fill factor of the cells decreased with increasing illumination intensity [7]. The decrease in the fill factor was attributed to photogenerated space charge that was generated in the cells, which screened the applied electric field, reducing the internal field of the solar cell and negatively affecting its properties [7]. This photogenerated space charge is the photocapacitance, and was measured in these previous experiments to explore the internal field structure of the solar cell. In my case the photocapacitance was used to extract the charge carrier drift mobilities in the CdTe solar cell samples.

4.1 Photocapacitance

Capacitance is a fundamental quantity in physics which describes an object's ability to hold electric charge. In general, capacitance is related to the geometry of the object, as well as the total amount of charge contained by the object. In essence then, photocapacitance is a measure of the charge in a material or object generated by incident light, the photogenerated charge. Specifically, photocapacitance is the measured response of photogenerated space charge to an applied voltage, where space charge is a continuum of electric charge distributed over a region of space [7]. It is the most direct measurement method addressing the charge profile of a solar cell. In terms of the measurement itself, the photocapacitance is defined as the difference

Figure 4.1: An illustration of the photocapacitance technique. In the dark conditions on the left, little to no space charge is generated. On the right, under illumination from the left, the drifting carriers create a space charge during their transit time. The change in the dark and light capacitances, ΔC here, is measured, and is equivalent to the photocapacitance.

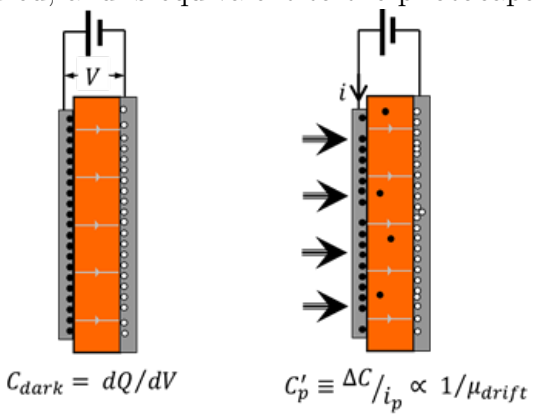

between the dark capacitance and the capacitance under illumination

$$C_p = C_{light} - C_{dark} \tag{4.1}$$

[2].

But how exactly does the photocapacitance provide this means of probing the internal field of the solar cell while at the same time accurately measuring charge carrier drift mobility? Well, we know that the E field in the CdTe solar cell needs to be strong enough to accelerate the carriers across the i-layer so that a majority of them can be extracted as current. If not, many of the carriers will drift throughout the i-layer, creating the photogenerated space charge which dampens the internal electric field. This is the precise quantity which the photocapacitance measures. Additionally, since the internal field strength is related to the drift mobility and the photogenerated charge present, the drift mobility can be related to the photocapacitance, as shown in Figure 4.1.

For my measurements of photocapacitance I used a quantity called the *linear photocapacitance* C_p' in order to extract mobilities. The linear photocapacitance is defined as the ratio of the photocapacitance measured at a

Figure 4.2: A measurement of the intensity dependence of the capacitance for a CdTe cell. The intensity is measured by the photocurrent of the sample at a -1 V bias.

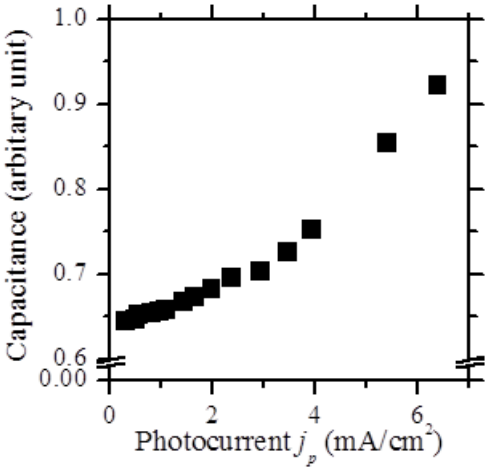

reverse bias potential to the photocurrent flowing through the solar cell

$$C'_p = \frac{C_p}{i_p} \tag{4.2}$$

In previous work with amorphous silicon solar cells, the linear photocapacitance decreased quickly with increased reverse bias voltage. This makes sense because under reverse bias conditions the carrier transit times across the solar cell will decrease, resulting in less stored photocharge to be measured by the photocapacitance measurement [5]. However, the above definition for linear photocapacitance is only valid for illumination intensities low enough that they do not disturb the dark E field profile inside the solar cell [5]. This is because the space charge of the moving photocarriers inside the sample increases with the illumination intensity. This can be shown by measuring the capacitance of the CdTe sample under short circuit conditions for different light intensities. It is important to note that the photocurrent of the solar cell is proportional to the incident light intensity if the spectral distribution of the light is not varied [3]. Figure 4.2 shows that for lower intensities, corresponding to photocurrents of less than 2 mA, the capacitance has a linear relationship with the intensity. This agrees with the conditions necessary to define the linear photocapacitance as we have in Equation 4.2. In this region, the photocurrent is small enough that the electric field can be taken to be

almost constant inside the sample. In the region after photocurrents of 2 mA, the capacitance increases nonlinearly with intensity, and this is where the space charge effects the internal field, possibly causing a collapse of the field.

Now that we have a basic understanding of what photocapacitance is, we can derive the equations necessary to use the method to determine drift mobilities. We know that photocapacitance measurements monitor the amount of space charge ΔQ in the solar cell, and if the ratio of the photocurrent to the photogenerated space charge is proportional to the drift velocity of the charge carriers, then

$$\Delta Q = \frac{d\, i_p}{2v} \tag{4.3}$$

where d is the thickness of the solar cell, i_p is the photocurrent, and v is the carrier drift velocity [2]. If ΔQ is low enough that it does not disturb the dark E field profile of the solar cell, then for uniform illumination throughout the sample the space charge is given by

$$\Delta Q = \frac{3}{2}\,\Delta C(V + V_o) \tag{4.4}$$

where ΔC is the photocapacitance (the change between the light and dark capacitances), V is the applied voltage, and V_o is the "offset voltage" [2]. The offset voltage comes from the built-in potential of the solar cell, which is approximately the difference in the Fermi levels of the p and n layers of the cell [2]. If we recall the definition of linear photocapacitance and that for a uniform field across the sample $E = \frac{V+V_o}{d}$, then the drift mobility can be related to the photocapacitance by the following relation:

$$\mu_D = \frac{v}{E} = \frac{d\, i_p}{2E\,\Delta Q} = \frac{d^2}{3C_p'\,(V + V_o)^2} \tag{4.5}$$

However, for Equation 4.5 the drift mobility is actually the combination of the drift mobilities of both carriers, electrons and holes, since the sample is being uniformly illuminated: $\mu_D = (\frac{1}{\mu_h} + \frac{1}{\mu_e})$. For surface illumination the drift mobility is of only holes, and Equation 4.3 changes from a factor of 3/2 to 1, resulting in the same equation for drift mobility as Equation 4.5 except with a factor of 1/2 instead of 1/3.

4.2 Methods

Recall that photocapacitance, from a measurement perspective, is simply the difference between the capacitance under illumination and the capacitance in the dark, as shown by Equation 4.1. The method I used to measure capacitances in the CdTe solar cell samples was direct lock-in detection of the current response of the solar cell to voltage modulation [2]. In other words, I used a function generator, a current amplifier, and a lock-in amplifier to detect the amplitude and phase of currents flowing in the solar cell [5]. A function generator, in the general sense, is an electronic device which generates various types of electrical waveforms over different frequencies. Both the type of waveform and frequency of the signal can be set manually or remotely on the device. The current amplifier is used to increase the current output measured from the solar cell, as it is typically very small. Finally the lock-in amplifier is used to detect and measure these small signals obtained from the current flowing through the solar cell, specifically the capacitance in the cell dot being measured.

The lock-in amplifier uses a technique called phase-sensitive detection to single out a component of a signal at a specific reference frequency and phase. This reference frequency is set by the input signal from the function generator, in my case a 1 kHz sine wave, and the lock-in detects the response of the experiment at that frequency. The frequency of the reference sine wave was chosen so that the time scale corresponded to complete charge collection across the cell, which in this case is about 1 millisecond. The lock-in amplifier has two channels for output signals: the X and Y channels. The X channel measures the "in-phase" component of the signal, which is not what we are trying to measure, so it is essentially ignored. The Y channel output from the lock-in amplifier is used to measure the "out-of-phase" component of the signal response. This is determined by the reactive components of the circuit, in this case the capacitance, which is given by

$$C = \frac{I}{\omega \bar{V}_m} \tag{4.6}$$

where I is the current produced by the lock-in voltage (the Y channel output from the lock-in), ω is the angular frequency of the reference signal, and $\bar{V}_m$ is the rms voltage of the sine wave reference signal. From the definition of angular frequency we know $\omega = 2\pi f$ where f is 1 kHz from the reference sine wave, and $\bar{V}_m$ is defined as $\bar{V}_m = \frac{V_{p-p}}{\sqrt{2}}$ where V_{p-p} is the peak-to-peak voltage

Figure 4.3: A full CdTe solar cell sample, viewed from the back or metal side. Each dot is denoted by its column and row, so the top left dot is named 11, under it is dot 12, etc.

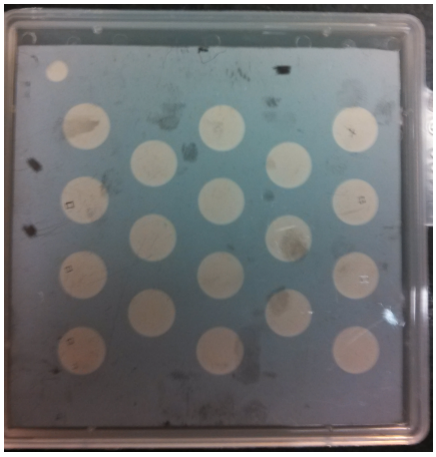

of the signal. Finally, the current I is dependent on the Y channel output of the lock-in amplifier and the sensitivity S of the current amplifier: $I = S \cdot Y$. So the final equation for the capacitance obtained from the lock-in amplifier is

$$C = \frac{S \cdot Y}{2\pi f \left(\frac{V_{p-p}}{\sqrt{2}}\right)} \tag{4.7}$$

This is what is used to calculate the linear photocapacitance in the sample, and thus the carrier drift mobility.

For the measurements themselves, I used various CdTe solar cell samples provided by First Solar, an industrial company that is at the forefront of CdTe solar cell technology. The samples I used for my measurements were predominantly bifacial, meaning that they could be illuminated from either the glass side or the metal side. Additionally, the solar cell samples have a designated layout for the back contacts. The dots are named by denoting each separate column of dots with a number from 1 to 5, increasing left to right across the sample, and rows 1 to 3 or 1 to 4 increasing from the top to the bottom of the sample. This layout is depicted in Figure 4.3. Some of these samples are different from others, as they may be created using slightly different processes, but more on that later.

For all of the solar cell samples I measured, I used a Newport Corporation Oriel Sol1A Class ABB solar simulator in Professor Schiff's lab to replicate

solar illumination on the samples. A solar simulator is a light source which is designed to produce light of the same spectral characteristics as the sun at various intensities. The light from a solar simulator is controlled in three dimensions: spectral content, spatial uniformity, and temporal stability. Each dimension is classified in one of three classes: A, B, or C, so the simulator I used had Class A spectral content and Class B ratings for the other two dimensions. I used different optical filters to change the illumination intensity and spectral profile seen by the samples. I used two different filters, a narrow band 550 nm green filter and an 830 nm red filter when illuminating the samples. The purpose of using these two filters is to measure different carrier mobilities as well as measuring different properties of the solar cell. The narrow band green filter is of a shorter wavelength, which does not penetrate fully into the thickness of the sample. This results in carrier generation produced from the green-filtered light being restricted mainly to the surface. Since under reverse bias only holes can drift across the CdTe sample and all of the carriers are being generated only on the illuminated surface, measurements using the green filter were used to measure hole drift mobilities. The red filter has a longer wavelength, allowing for light to fully penetrate uniformly into the sample, so properties of the bulk material can be measured. The red filter was used to take measurements of electron drift mobilities.

4.2.1 I-V Curve Measurement

Before taking the capacitance measurements, it is necessary to take an accurate measurement of the photocurrent produced in the solar cell to use in calculating the linear photocapacitance. This is obtained through a generic technique in the study of solar cells known as I-V curve measurement. The I-V curve is a measurement of the current and voltage characteristics of the solar cell, and under illuminated conditions will provide the photocurrent as a function of applied voltage. First a measurement of the current in dark conditions is taken to check for any current leakages in the cell dot, as a leakage of current would negatively affect any subsequent measurements. If the dot passes the dark current test, then a measurement of the photocurrent is taken, as the cell is illuminated by the solar simulator and the dot is placed underneath the optical filter being used for the measurement. The I-V curve measurement is performed by applying a reverse bias voltage to the solar cell

Figure 4.4: A block diagram of the experimental circuit for the I-V measurement.

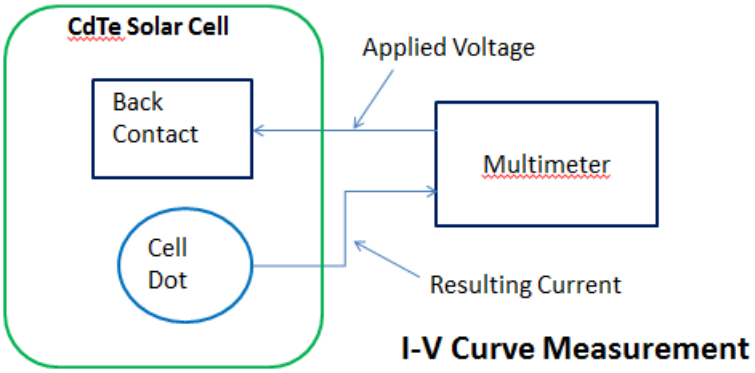

and measuring the resulting current from the cell dot. The voltage is applied to the solar cell through a conductive probe that is attached to the back contact, while the current through the dot is obtained by a similar probe that is attached to the dot itself. A multimeter records the applied voltage and the resulting current, both of which are stored in a text file that is saved upon completion of the experiment by a Labview program. A diagram of the experiment is shown in Figure 4.4.

The I-V curve measurement begins by attaching the solar cell to a platform, which is used to keep the cell in place and for convenience when taking measurements on both sides of the cell while keeping the overall circuit/connection intact. Next, the conductive probes are attached to their respective positions on the solar cell, the current probe to the cell dot being measured and the voltage probe to the back contact. Occasionally it is necessary to scratch off some of the back layer with a razor blade to get to the conductive portion of the cell. Once the probes are attached, their cables are plugged into the multimeter and the Labview program is opened. In the program, the voltage range for the I-V curve, the step size of each voltage increase, and many other parameters are set before the experiment runs. The voltage range I typically used was from -2 V to 0.8 V in steps of 0.02 V.

First the dark current measurement was performed, so it was necessary to cover the solar cell with a black sheet to minimize its light exposure. After the dark current was measured, and if there was minimal leakage current, the solar simulator would be turned on and whichever optical filter was be-

ing used for the experiment would be placed above the cell dot to filter the incoming light from the solar simulator. For measurements on the glass side of the solar cell, the box containing the filter could be placed directly on the solar cell, while for measurements on the metal side it needed to be elevated above the cell to avoid interfering with the current probe attached to the dot. An important note is that if the incident light intensity on the dot is too high, the photocurrent will not be relatively constant at reverse bias, which is necessary for a good capacitance measurement. In this vein, different neutral optical filters were used to decrease the incident intensity, and were added to the apparatus which held the red or green filter accordingly. Finally the photocurrent was measured and recorded for use in calculating the linear photocapacitance.

4.2.2 Photocapacitance Measurement

Once the I-V curve tests are complete, the photocapacitance, or more specifically the light and dark capacitances, can be measured. The conductive probes that are attached to the solar cell do not change position, but the layout of the circuit behind them does. The connections are taken from the multimeter and attached to the function generator and the current amplifier. The circuit layout is such that the current being measured from the cell dot is now input into the current amplifier. The output from the current amplifier is then connected to the input port of the lock-in amplifier, whose output is connected to the input terminal of the function generator. Recall that the function generator creates a 1 kHz sine wave as the reference signal for the lock-in amplifier. Finally, the function generator also controls the voltage applied to the solar cell, so its output terminal is connected to the voltage probe on the back contact. A diagram of the measurement circuit is shown in Figure 4.5, which is also controlled by a Labview program. The program sets the voltage range as well as various parameters on the lock-in amplifier such as the sensitivity and time constant. For most of my capacitance measurements I used a voltage range from -2 V to 0.3 V, measuring in increments of 0.1 V. If the dark current characteristics were better for a different range of voltages, I would adjust my measurement accordingly. I measured the dark capacitance first, and then the light capacitance under illumination and with the necessary filters. These values were recorded by the Labview program and stored in a text file. The measurements were performed using both red and green filters on the glass and metal sides of various solar cell samples.

Figure 4.5: A block diagram of the experimental circuit for the photocapacitance measurement.

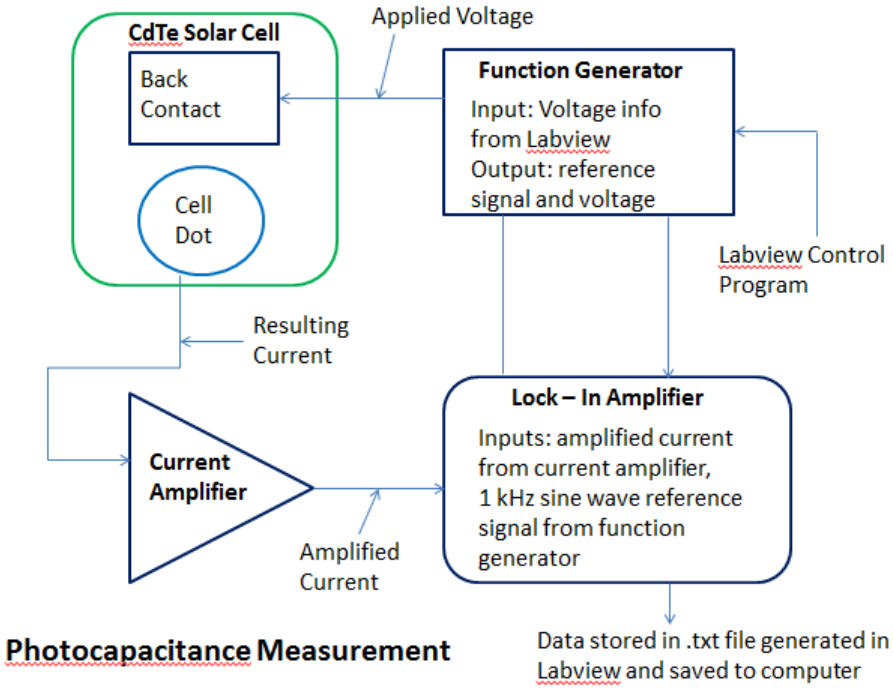

4.3 Analysis

I performed the data analysis for my experiments in a program called Origin, a software application for data analysis and high-quality graphing. I would input the applied voltage values from the capacitance measurement (usually from -2 V to 0.3 V), and the Y channel values from the lock-in amplifier data for the light and dark capacitance runs of the experiment into Origin. These values are in millivolts, so they are multiplied by 10^{-3} to obtain values in volts, and then put into Equation 4.7 to determine the light and dark capacitance values. During the experiments, the amplifier sensitivity and the reference signal peak-to-peak voltage are kept constant at 10^{-3} and 100 mV respectively. The photocapacitance is then calculated from the difference between the light capacitance and the dark capacitance, as shown in Equation 4.1. Then the photocurrent from the I-V measurement is entered so that the linear photocapacitance can be calculated at each applied voltage

using Equation 4.2. The bias or offset voltage, necessary for calculating the drift mobility as shown in Equation 4.5, is calculated from a plot of $\frac{1}{C_d^2}$ vs. Voltage where C_d is the dark capacitance. The bias voltage is given by the x-value of the point of intersection between the curve and the x-axis. Finally, the thickness of the i-layer d of the sample is calculated using a parallel plate capacitor model for the solar cell, where

$$C = \frac{\epsilon\epsilon_0 A}{d} \tag{4.8}$$

and solving for d yields

$$d = \frac{\epsilon\epsilon_0 A}{C} \tag{4.9}$$

In Equation 4.8 and Equation 4.9 ϵ_0 is the relative permittivity of free space ($8.85 \cdot 10^{-14} \frac{F}{cm^2}$), ϵ is the dielectric constant for CdTe (≈ 11), and A is the area of a cell dot (1.1 cm^2).

To calculate the drift mobility obtained from a photocapacitance measurement, it is important to note with which filter and on which side of the solar cell sample the measurement was taken. For surface illumination where the green 550 nm filter was used, Equation 4.5 with the changes described in Section 4.1 is used to determine the hole drift mobility. This equation is put into a script in Origin that takes the input parameters of thickness d, applied voltage V, bias voltage V_o, and linear photocapacitance C_p' and calculates the value of the drift mobility for that particular data set. Once the hole drift mobility has been calculated, the data from the uniform illumination of the sample, or use of the red 830 nm filter, is used to determine the electron drift mobility. Equation 4.5 is fit in the same way as the equation for the holes with the additional fit parameter of the hole drift mobility. The results of these mobility calculations are shown in the next section.

Chapter 5

Results

I made various measurements of different CdTe thin film solar cells provided to our research group by First Solar. When I was first making measurements to understand how the technique works and hone my skills, I measured many older samples which did not have bifacial characteristics. However, for the

Figure 5.1: Dark capacitance data from sample F3 dot 51 that was used to find the bias voltage V_{bi}. Approaching forward voltage values results in a drop in $\frac{1}{C^2_{dark}}$, and its intersection with the x-axis is the bias voltage used for calculating the mobility of the carriers in the dot.

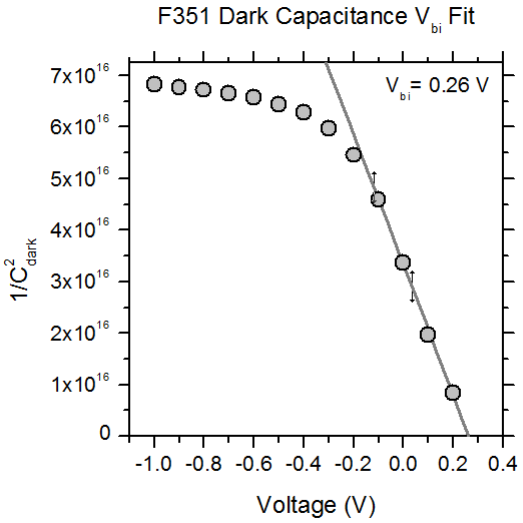

Figure 5.2: A measurement of the carrier drift mobilities in sample F3 dot 51. As shown in the legend, the filled in circles represent measurements from the glass side of the sample and the open circles represent metal side measurements.

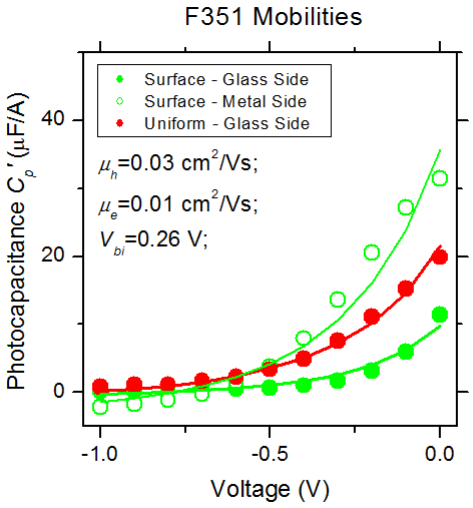

majority of my experimental work I measured bifacial CdTe samples from both sides under surface and uniform illumination. The processes described in Sections 4.2 and 4.3 were used to take the measurements and analyze the data. Examples of this are shown in Figure 5.1 and Figure 5.2. Figure 5.1 shows a linear fit of the dark capacitance data to determine the bias voltage for that particular cell dot. Again, this is used to calculate the drift mobility. Figure 5.2 shows the voltage-dependent photocapacitance measurements for different types of illumination on the same sample.

The samples themselves were slightly different, as some were chemically treated during the development of the solar cell while others were not. The specifics of the treatment process were not revealed to us during the experiments. My measurements primarily focused on dots from two samples, an untreated sample called I3 and a treated sample called F3. The overall magnitudes of the mobilities I obtained were in the same general value range, between 10^{-2} and 1 cm^2/V$\cdot$s. Recall that typical mobilities for single crystal CdTe are on the order of $100 - 1000$ cm^2/V$\cdot$s. However, between the two kinds of samples, the relative carrier mobilities were reversed. In the treated F3 sample the electron mobilities were lower than the hole mobilities, while

Figure 5.3: A measurement of the carrier drift mobilities in sample I3 dot 53. The green measurements were surface illuminated, using the green filter, while the red was uniformly illuminated using the red filter.

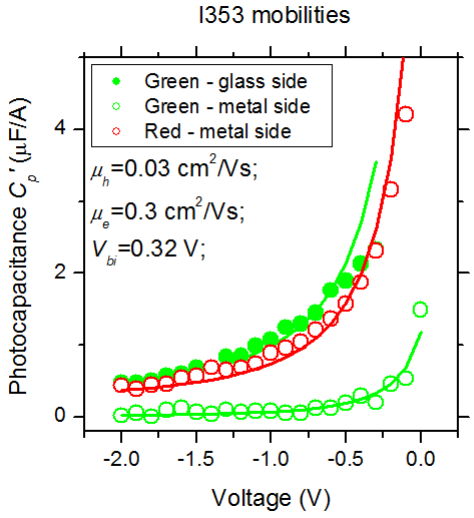

in the untreated I3 sample it was the reverse case. This is shown in Table 5.1 and Figure 5.4, which compare the electron and hole drift mobilities in the dots that I measured from both samples. The mobility measurements for individual dots are shown in the appendix.

Table 5.1: Summary table of all measured mobilities.

Sample	Dot	Hole Mobility (cm^2/Vs)	Electron Mobility (cm^2/Vs)	Bias Voltage (V)
F3	51	0.03	0.01	0.26
F3	52	0.3	0.18	0.2
F3	54	0.1	0.07	0.27
I3	43	0.1	1	0.28
I3	51	0.03	0.4	0.26
I3	52	0.075	0.3	0.32
I3	53	0.03	0.3	0.32
I3	54	0.065	0.35	0.27

Figure 5.4: A summary plot of the drift mobilities measured from the I3 and F3 samples. Fewer dots on the treated sample were measured due to poor dark current characteristics such as leakages. The mobilities are plotted on a log-log scale.

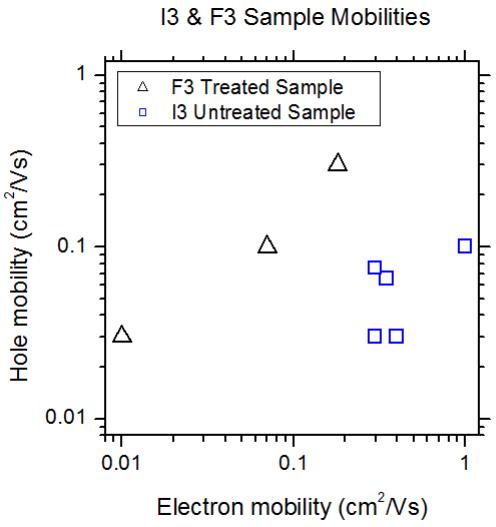

Chapter 6

Conclusions & Future Work

Recall from Figure 1.1 that the drift mobilities in thin film CdTe are many orders of magnitude smaller than those in single crystals. My measurements of the drift mobilities in CdTe thin film solar cells using photocapacitance aimed to shed some light on this discrepancy, which could change how solar cell manufacturers model the devices they are making. The measurements that I took, summarized in Table 5.1 and Figure 5.4, are further evidence of a drastic difference in carrier drift mobilities between thin film and single crystal CdTe. This means scientists and engineers who model thin film CdTe solar cells have been using incorrect assumptions for the carrier drift mobilities. Usually their models incorporate the drift mobilities found in single crystals of CdTe, while my data contributes to the notion that these values are incorrect. This evidence is found in Figure 6.1, which contains all of the photocapacitance measurements of drift mobilities performed by our research group. A majority of these measurements result in carrier drift mobility values on the order of 1 $cm^2/V \cdot s$ or less, which again is at least 3 orders of magnitude less than values measured in single crystals.

In terms of addressing the reasons behind this mobility discrepancy, that is dependent on the prevailing theory used to describe the drift mobilities. The theory that was used and outlined in this project is the effective mass theory - that the drift mobilities have a relationship with the effective mass of the carrier. Though this theory has been extremely successful in describing carrier behavior in various materials over the last 50 years, it may not accurately describe charge transport in thin film CdTe. To check that a particular model makes sense for a material, usually measurements of the temperature dependence of the drift mobilities are needed. Though I was unable to make

Figure 6.1: A summary plot of all of the photocapacitance measurements on CdTe performed by Professor Schiff's research group, including my own.

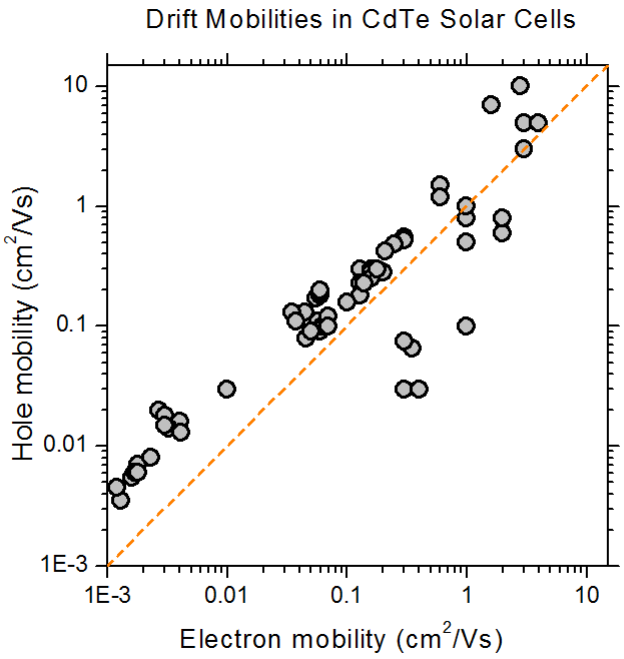

these kinds of measurements, preliminary evidence from the graduate student I have been working with, Qi Long, suggest that the carrier mobilities in CdTe are weakly temperature dependent. However, this weak dependence is not enough to account for the large mobility difference between thin film CdTe and single crystals.

Though my photocapacitance measurements of drift mobilities in CdTe solar cells have not directly addressed the reasons behind the mobility discrepancy, they have added to the knowledge base of evidence supporting that this discrepancy exists. I have contributed to the idea that device modelers need to re-evaluate how they model the carrier mobilities in thin film CdTe solar cells, which can have important impacts on device fabrication and performance. In the future, with more temperature dependence measurements of photocapacitance, as well as new theories describing carrier transport in thin films, hopefully this discrepancy can be accurately addressed. Understanding the reasons behind this mobility difference may lead to more optimized solar cells with better open circuit voltage characteristics.

Bibliography

[1] N.W Ashcroft and N.D. Mermin, *Solid State Physics*, Holt, Rinehart and Winston, New York, Chapters 1-3, 8-9, 12, (1976)

[2] J.-K. Lee, A.M. Hamza, S. Dinca, Q. Long, E.A. Schiff, Q. Wang, B. Yan, J. Yang, S. Guha, *Drift-mobility characterization of silicon thin-film solar cells using photocapacitance*, Journal of Non-Crystalline Solids, Volume 358, Issue 17, 1 September 2012, pp. 2194-2197

[3] E. Lorenzo, *Solar Electricity: Engineering of Photovoltaic Systems*, Prognesa Publishing, Sevilla, Spain, Chapter 2, (1994)

[4] Antonio Luque, Steven Hegedus, *Handbook of Photovoltaic Science and Engineering*, John Wiley, 2nd Ed., Chapter 14, (2011)

[5] Indra Nurdjaja, and E. A. Schiff, *Photocapacitance and Hole Drift Mobility Measurements in Hydrogenated Amorphous Silicon (a-Si:H)*, Materials Research Society Symposium Proceedings, Vol.467, Pittsburgh, 1997, pp. 723-732

[6] John Singleton, *Band theory and electronic properties of solids*, Oxford University Press, Chapters 1-3, 5, 9, (2001)

[7] Qi Wang; Crandall, Richard S.; Schiff, Eric A., "Field collapse due to band-tail charge in amorphous silicon solar cells," *Photovoltaic Specialists Conference, 1996., Conference Record of the Twenty Fifth IEEE ,* pp.1113-1116, 13-17 May 1996

Appendix A

More Mobility Measurements

Figure A.1: A measurement of the carrier drift mobilities in sample F3 dot 52.

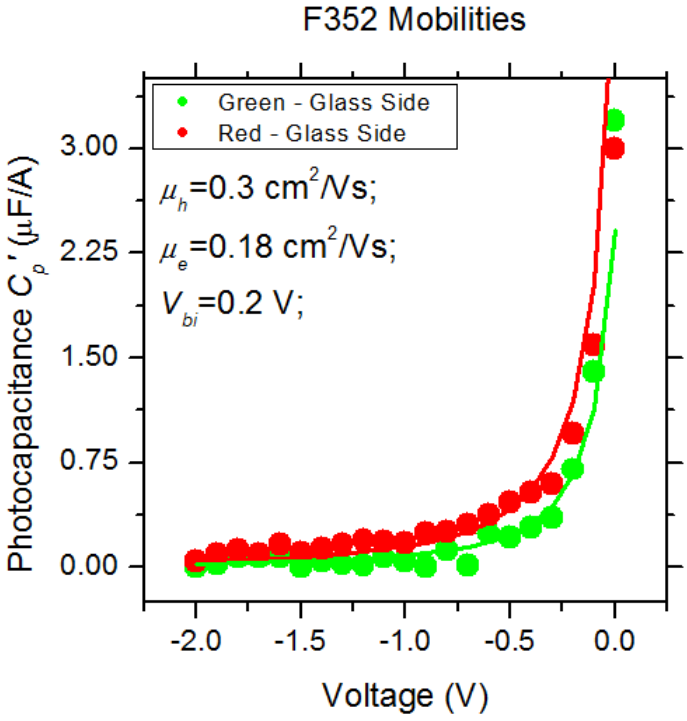

Figure A.2: A measurement of the carrier drift mobilities in sample F3 dot 54.

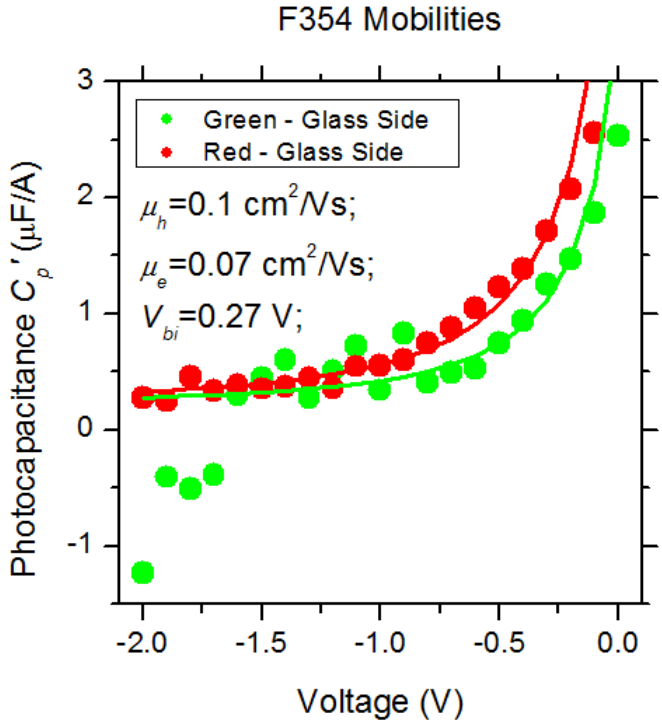

Figure A.3: A measurement of the carrier drift mobilities in sample I3 dot 43.

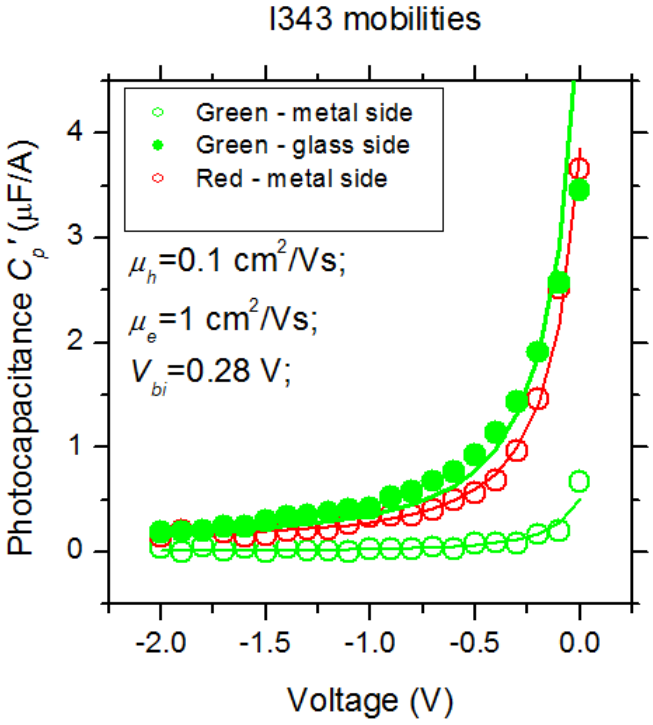

Figure A.4: A measurement of the carrier drift mobilities in sample I3 dot 51.

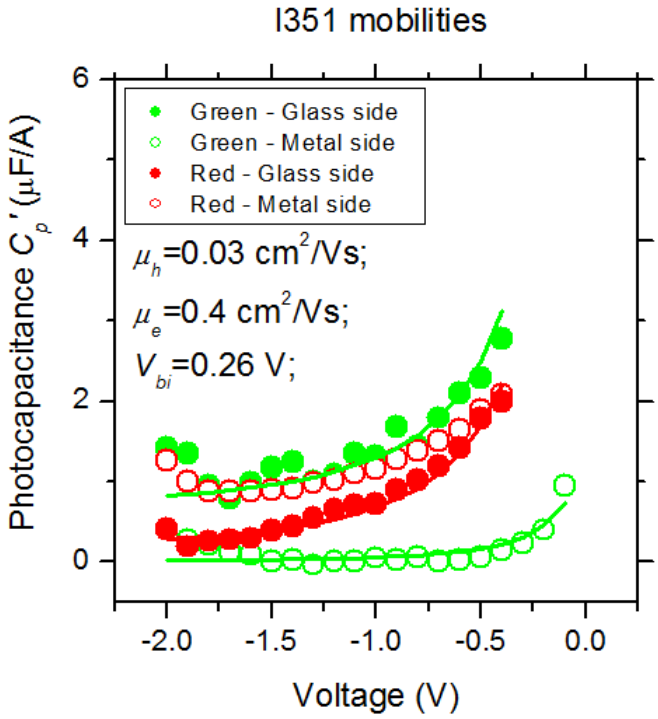

Figure A.5: A measurement of the carrier drift mobilities in sample I3 dot 52.

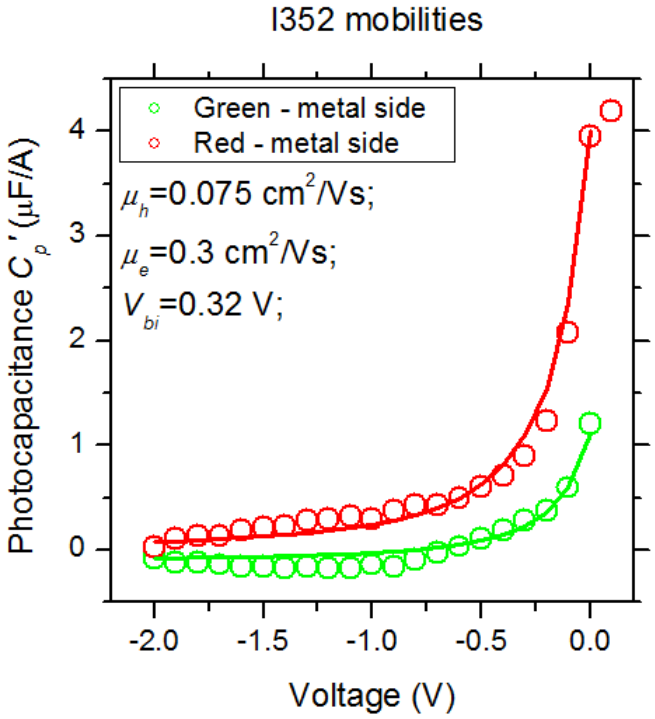

Figure A.6: A measurement of the carrier drift mobilities in sample I3 dot 54.